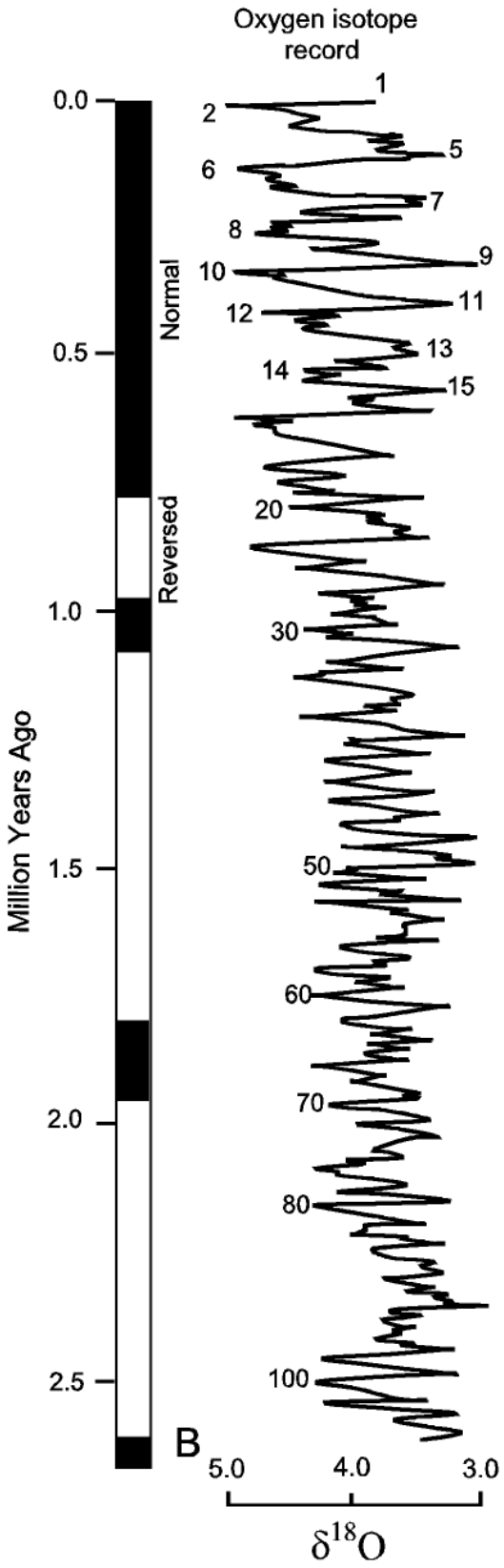

Figure 60: Quaternary climate. Oxygen isotope curve from ODP site 677 showing numbering of selected stages to 2.5 Ma. The column on the left shows the palaeomagnetic time scale. After NJ Shackleton *et al.* (1995) (adapted from Chiverrell and Thomas 2006)

Figure 61: The glaciation of Britain. The palaeogeography of Britain during the Devensian glaciation (*circa* 75-15 ka), showing source areas, flow directions and maximum limit and major retreat stages (adapted from Chiverrell and Thomas 2006)

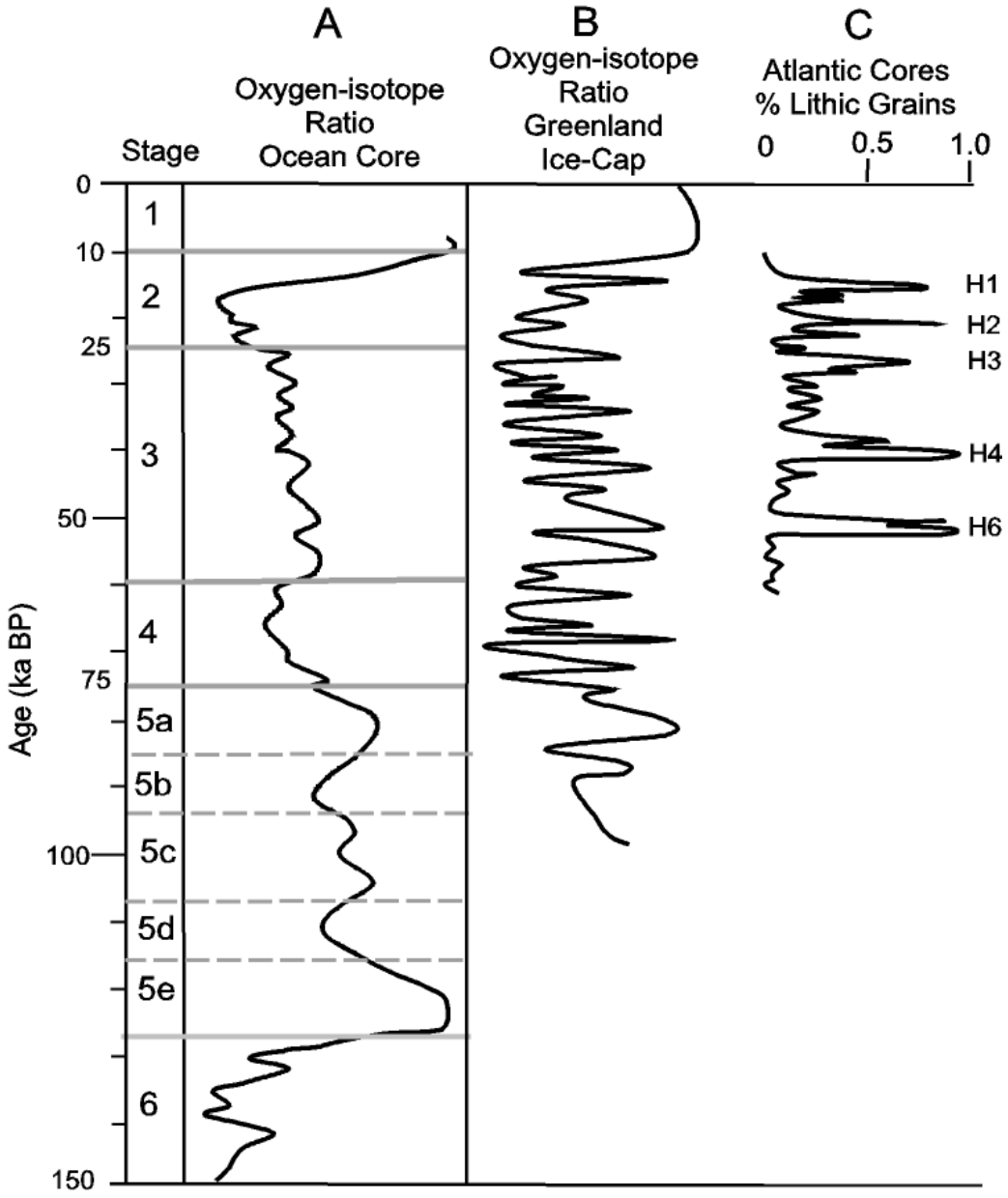

Figure 62: Climate during the last 150,000 years. (a) Marine oxygen isotope curve for the last 150 ka. (b) Oxygen isotope curve from the Greenland Ice Cap. (c) Heinrich events indicated by lithic grains in the northern Atlantic marine cores (adapted from Chiverrell and Thomas 2006)

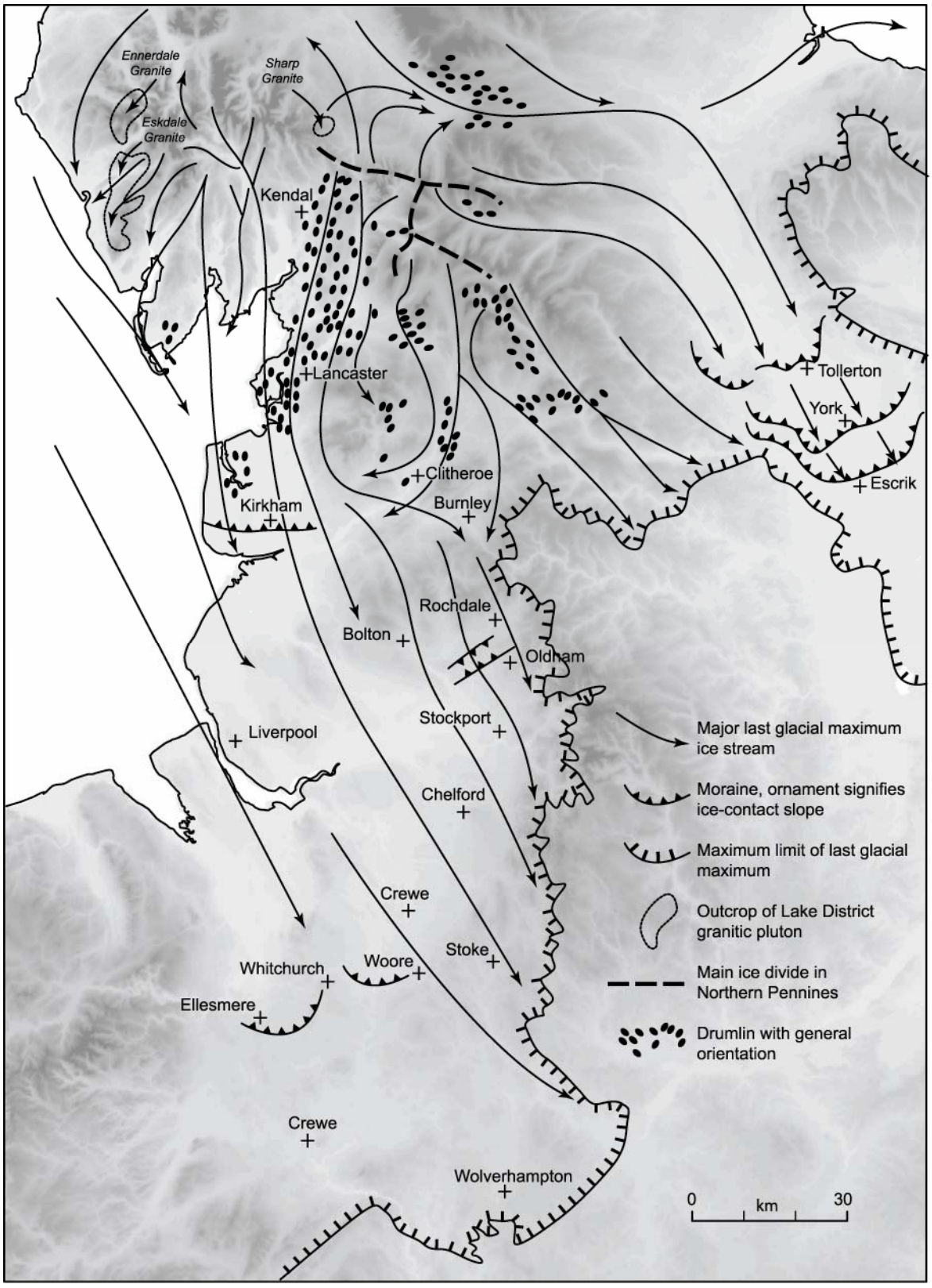

Figure 63: The Devensian glaciation of north-west England. The palaeogeography during the Devensian glaciation (*circa* 75-15 ka), showing source areas, flow directions, ice divides and drumlin fields over ground topography (adapted from Crofts 2006) (© Ordnance Survey)

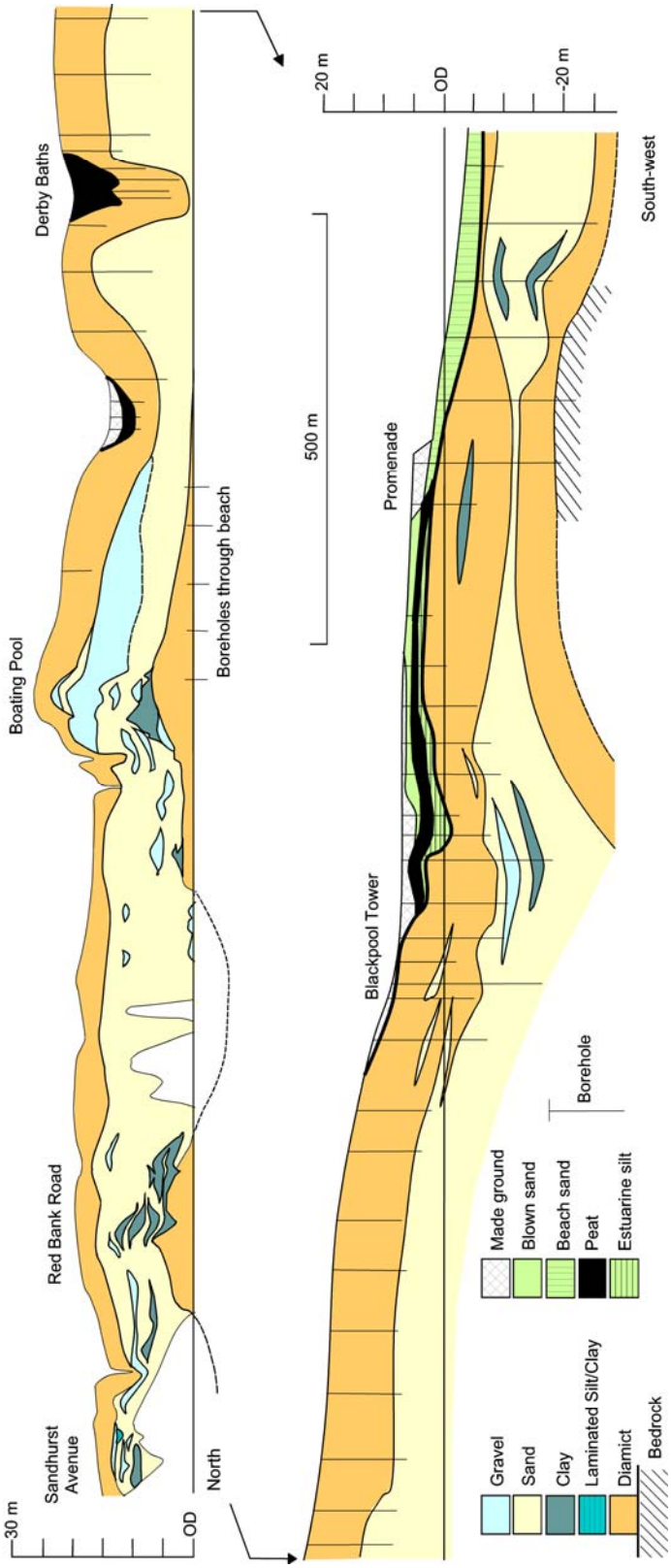

Figure 64: Coastal sections at Blackpool from the researches of Binney (1855) and De Rance (1877a) redrawn by Wilson and Evans (1990) and a recompilation of the boreholes through Blackpool against a topography derived from the NextMAP DEM (redrawn from Wilson and Evans 1990)

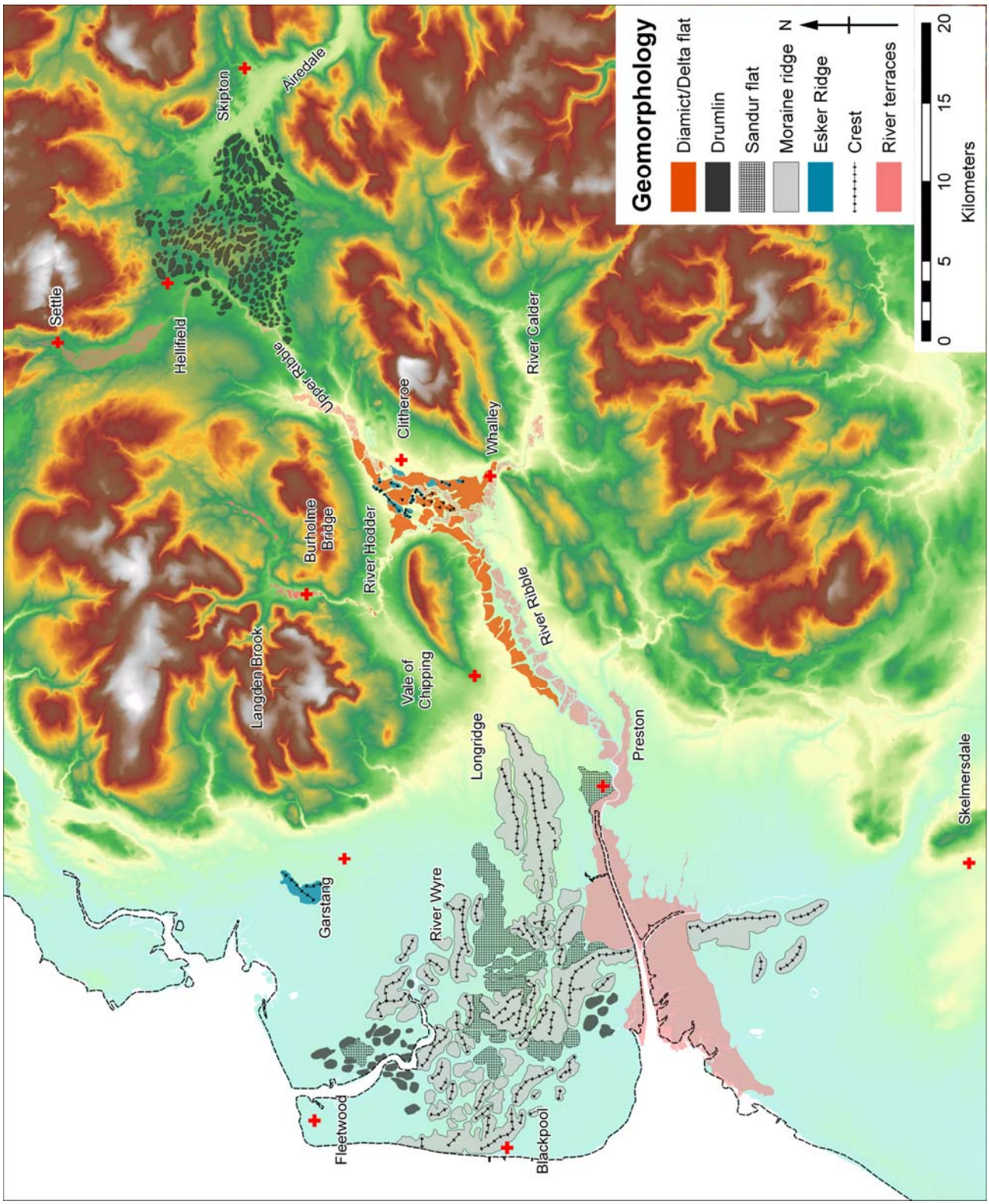

Figure 65: Geomorphology of the Ribble catchment and distribution of major locations (© Ordnance Survey)

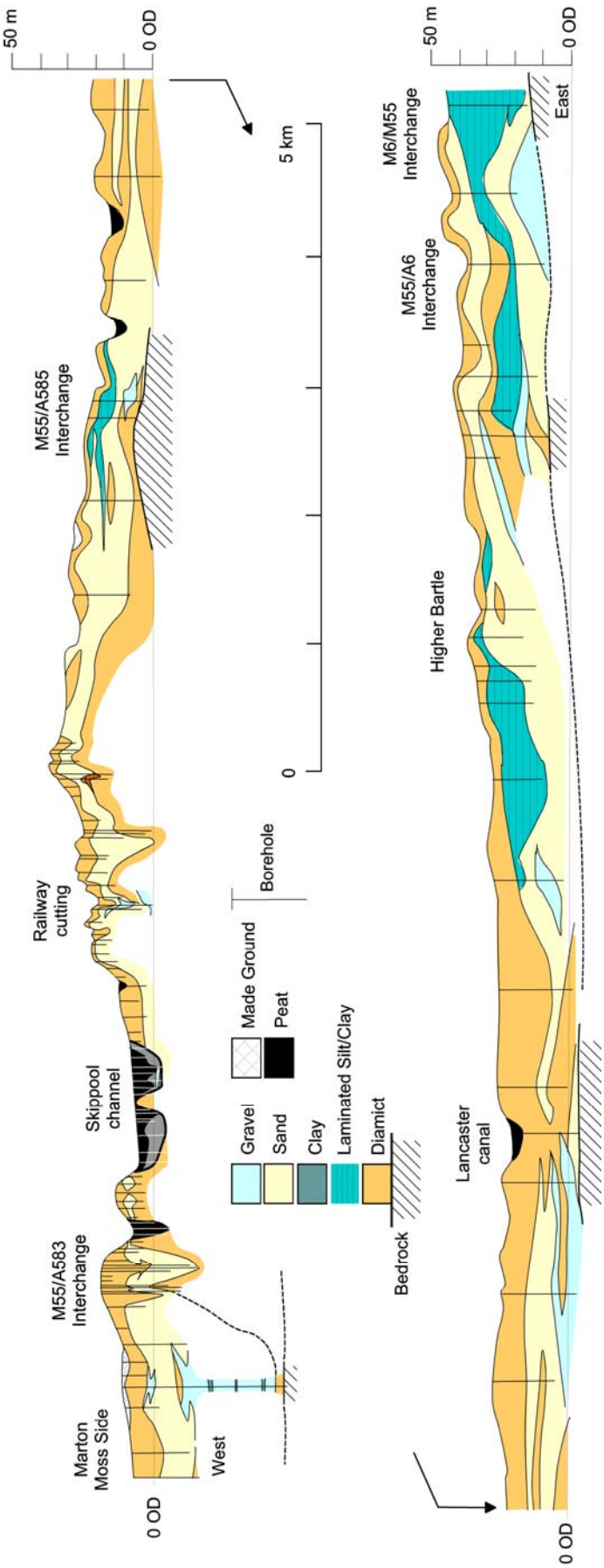

Figure 66: Re-analysis of the M55 borehole series presented by Wilson and Evans (1990) and Aitkenhead *et al* (1992), plotted against a topography derived from the NextMAP DEM

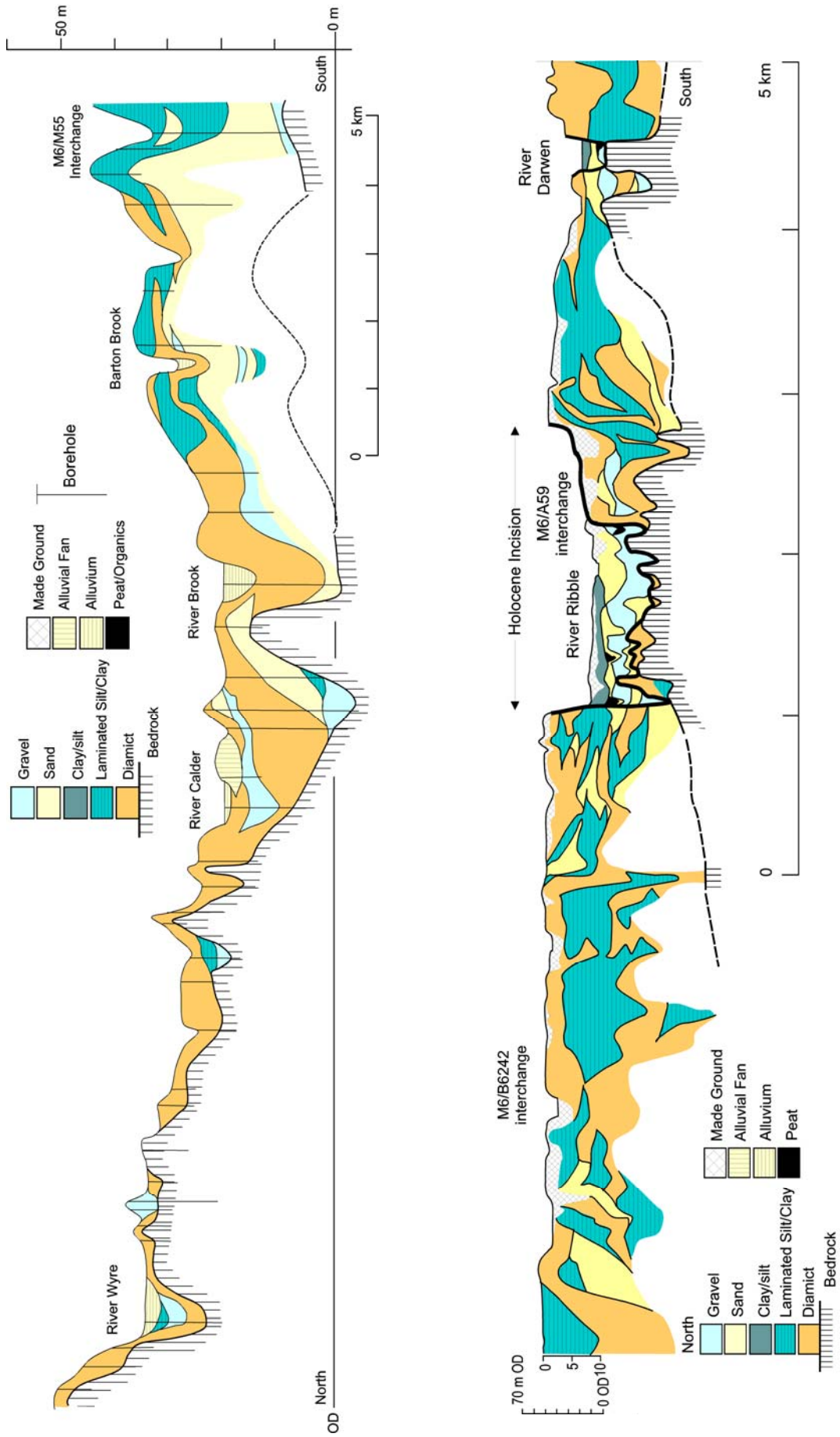

Figure 67: Re-analysis of the M55 borehole series presented by (Wilson and Evans 1990; Aitkenhead *et al* 1992), plotted against a topography derived from the NextMAP DEM

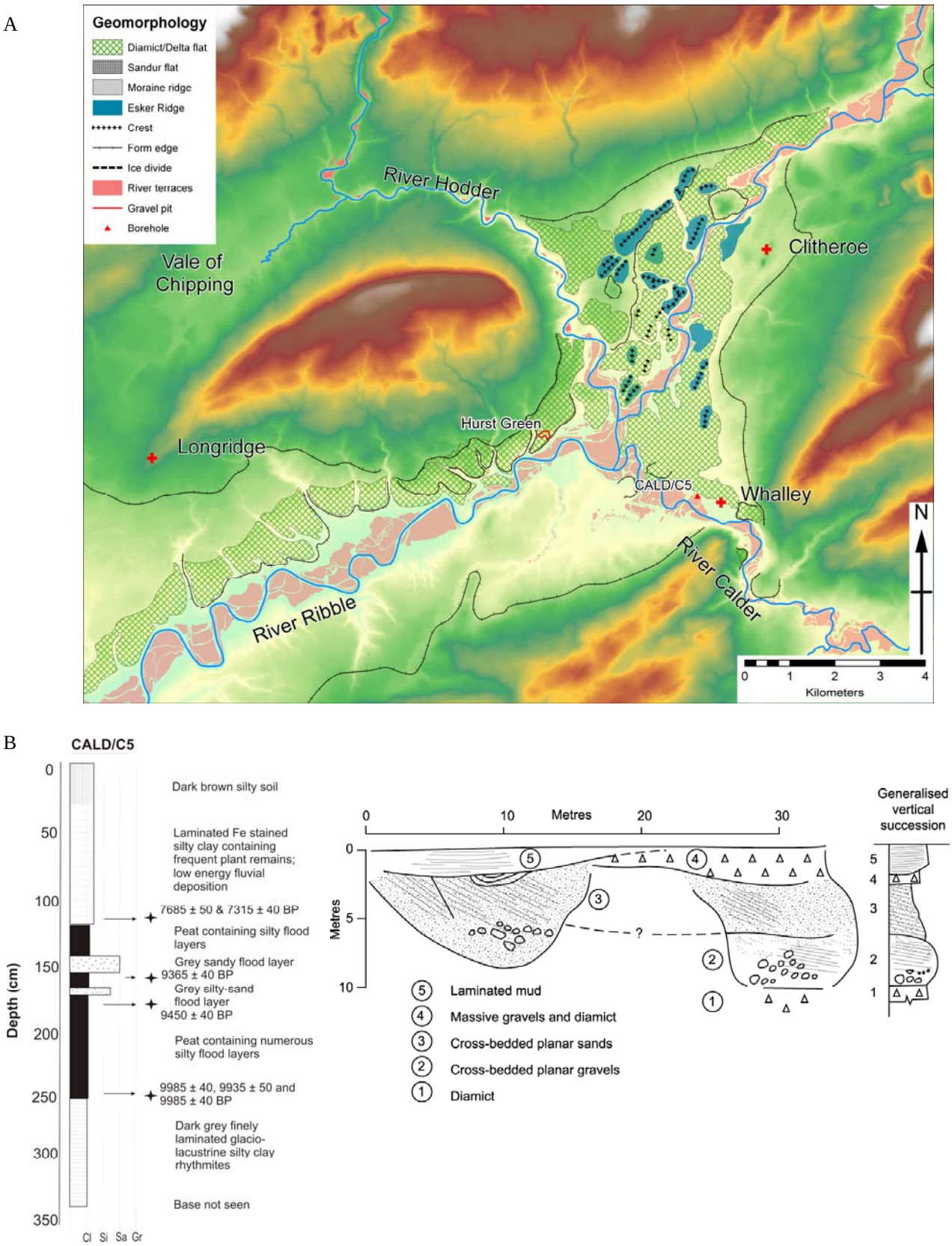

Figure 68: A) Geomorphology of the region to the west of Clitheroe near the confluences of the Ribble, Hodder and Calder (© Ordnance Survey); B) A borehole sequence from the lower Calder and the deltaic sediments exposed in a former gravel working at Hurst Green

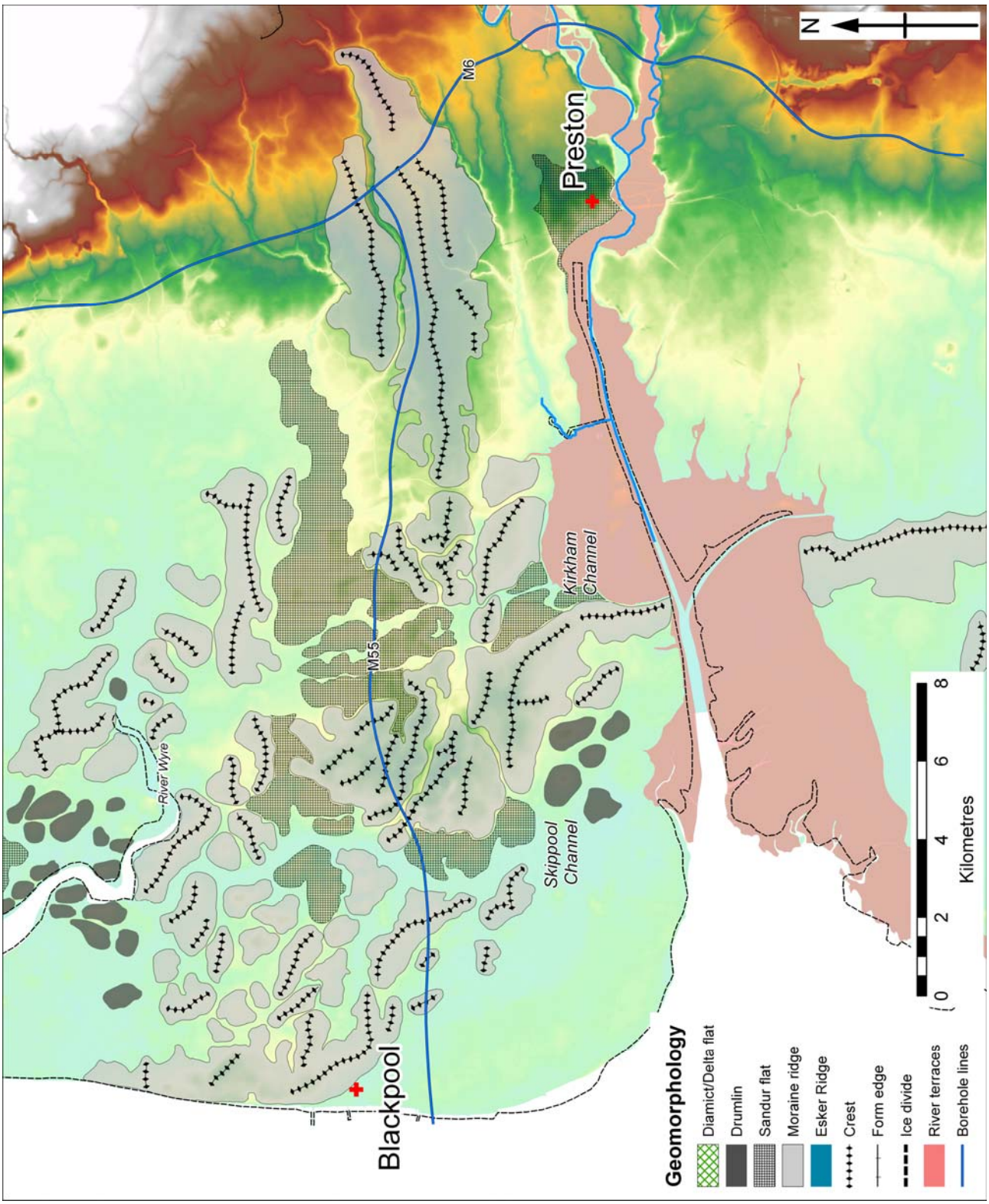

Figure 69: Geomorphology of the Kirkham moraine complex between Preston and Blackpool, which highlights the location of the M6 and M55 borehole series (© Ordnance Survey)

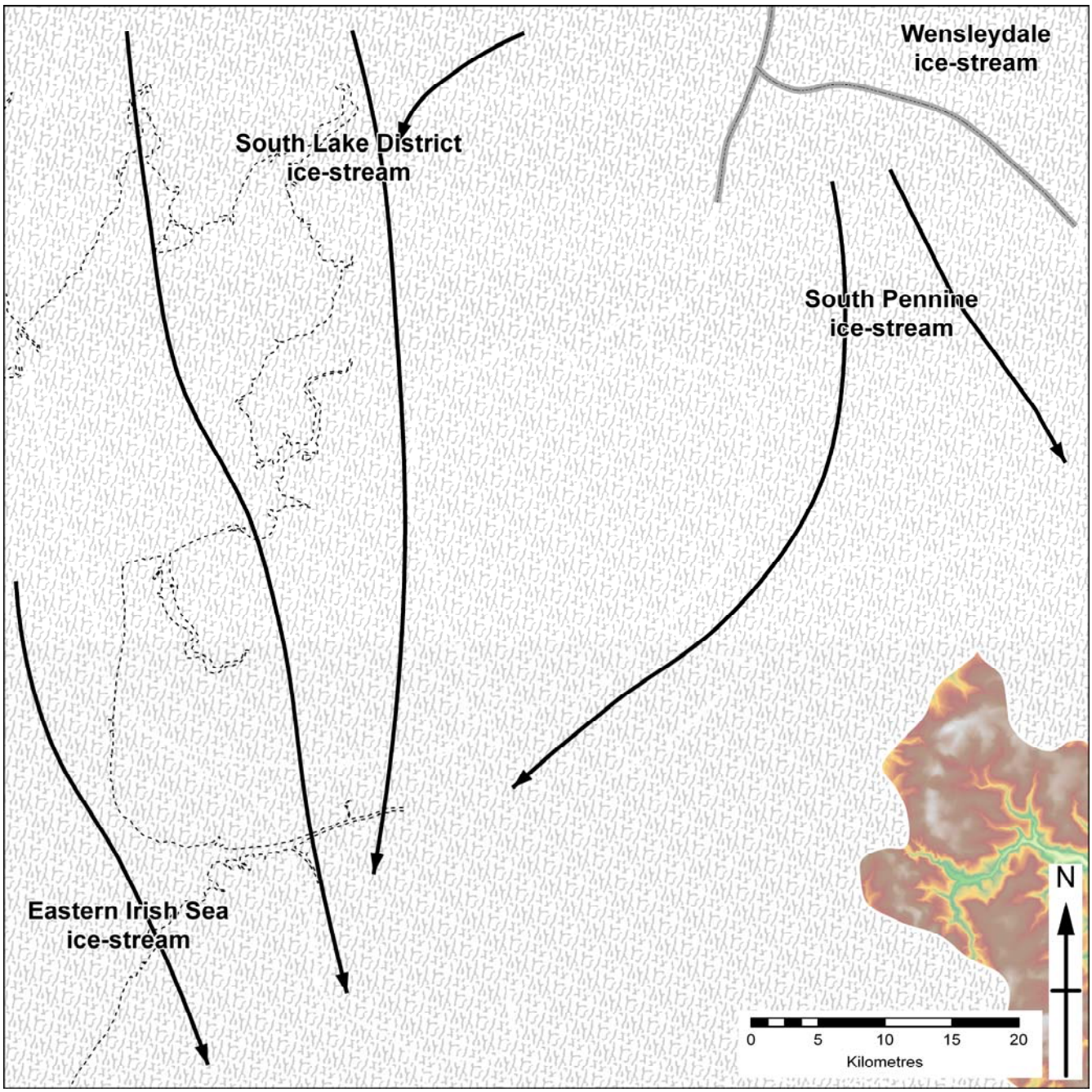

Figure 70: Ice cover and ice stream flow direction in the Ribble basin during Heinrich event 2, the late Devensian glacial maximum (© Ordnance Survey)

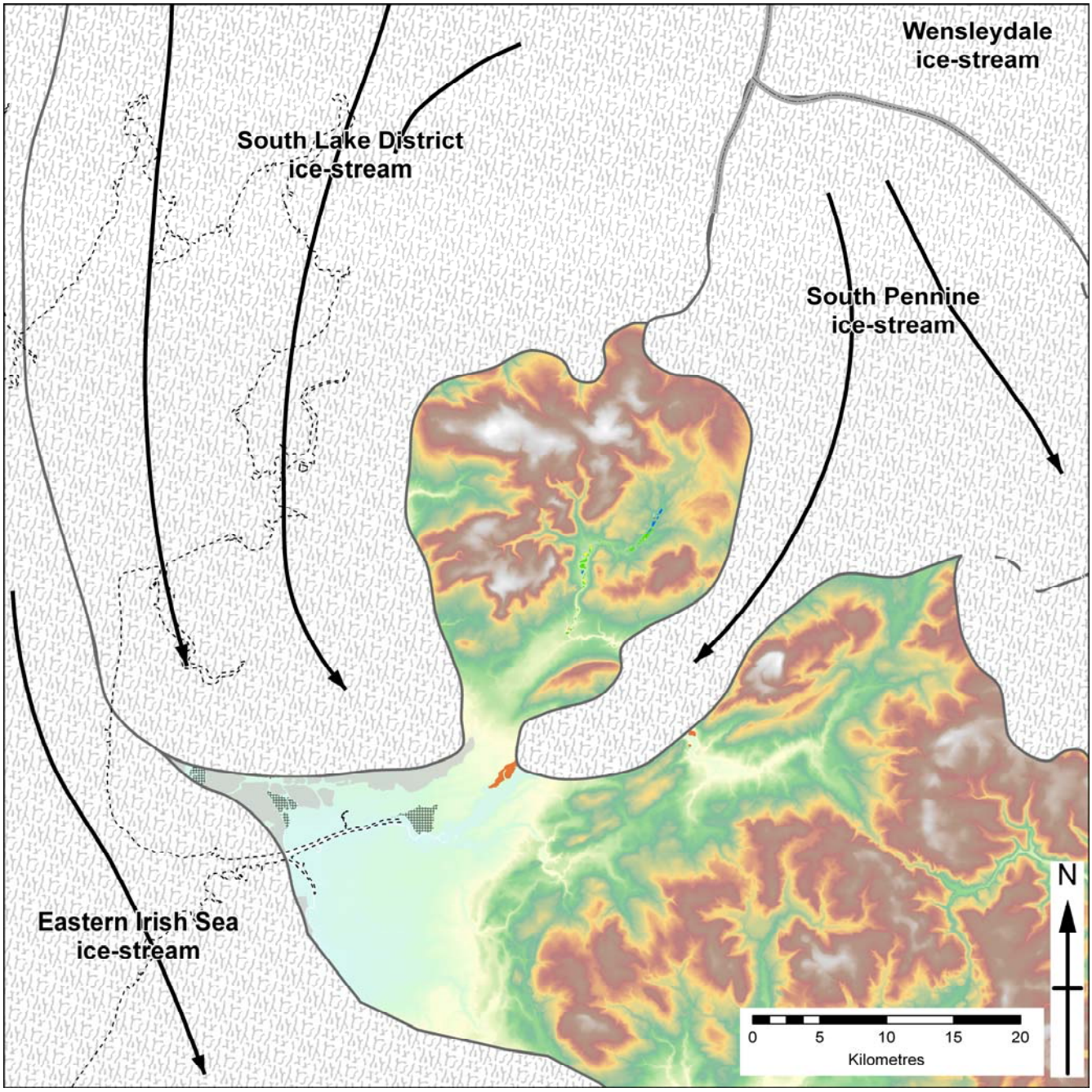

Figure 71: Ice cover and ice stream flow direction in the Ribble basin during the retreat from Heinrich event 2 limits, with a large free basin in the lower Ribble that contained an ice-dammed lake (© Ordnance Survey)

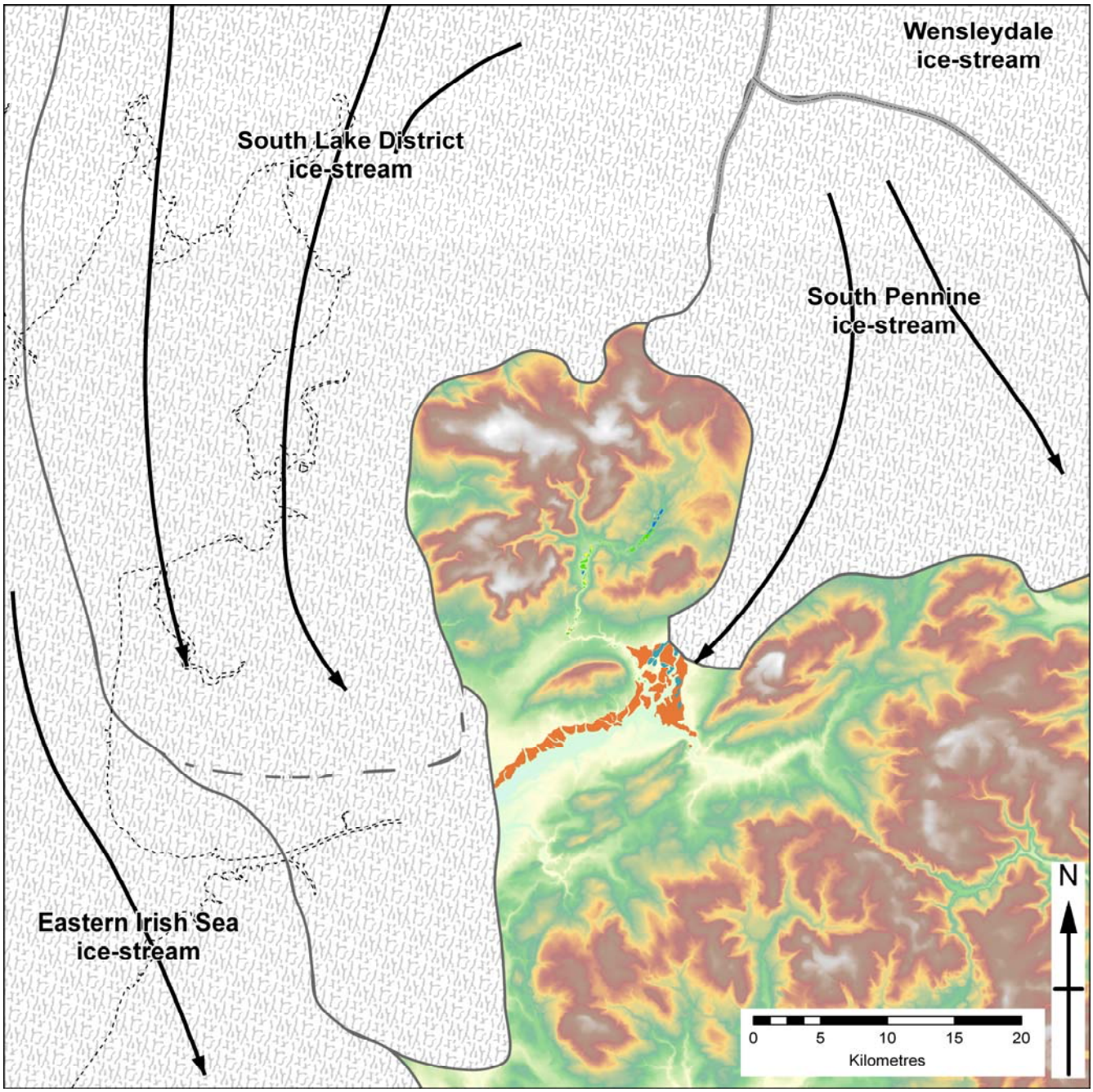

Figure 72: Alternative configuration of ice cover and ice stream flow direction in the Ribble basin during the retreat from Heinrich event 2 limits, with a large free basin in the Lower Ribble that contained an ice-dammed lake (© Ordnance Survey)

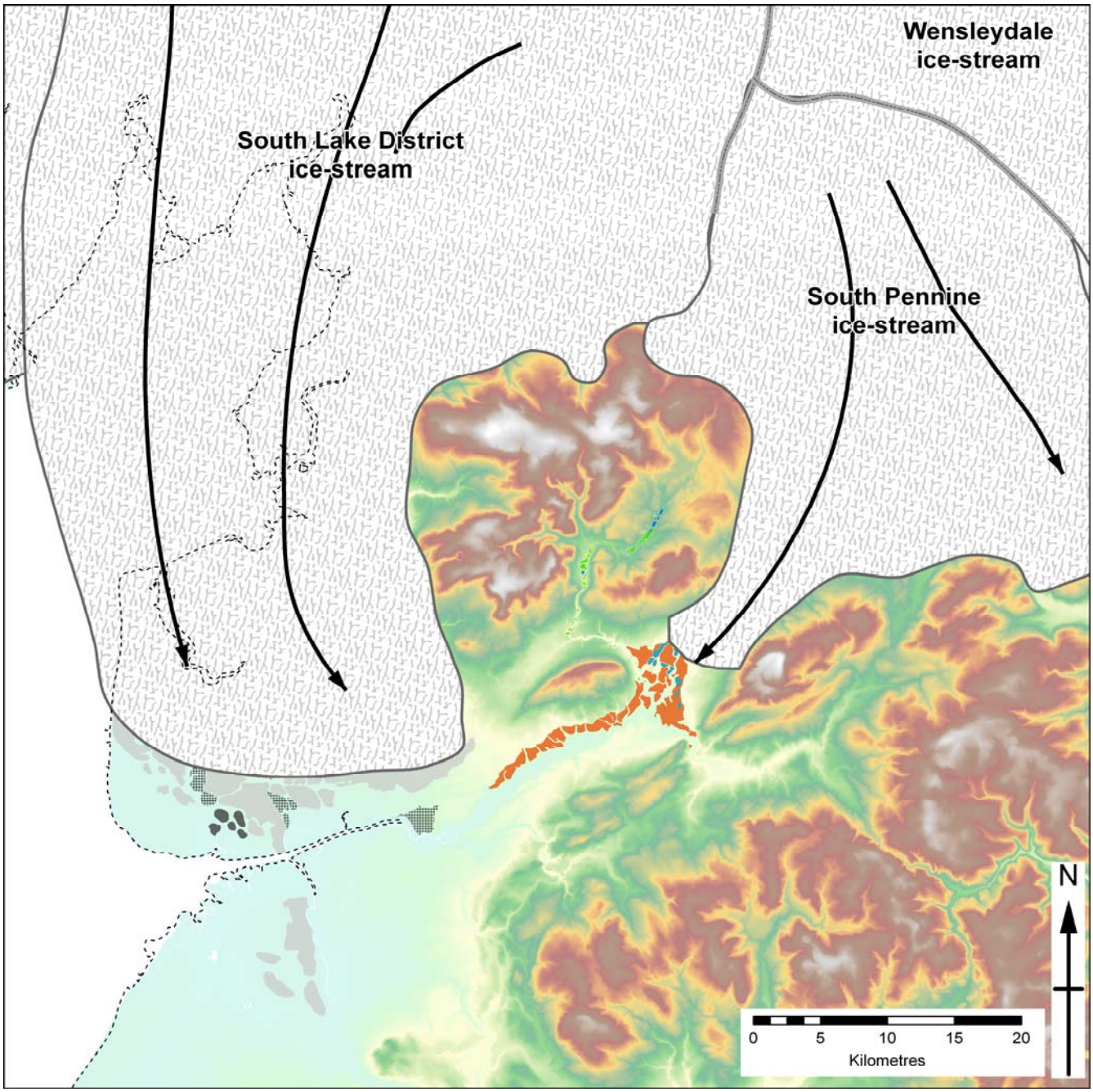

Figure 73: Possible ice cover and ice stream flow direction in the Ribble basin during rapid ice advance to Heinrich event 1 limits (© Ordnance Survey)

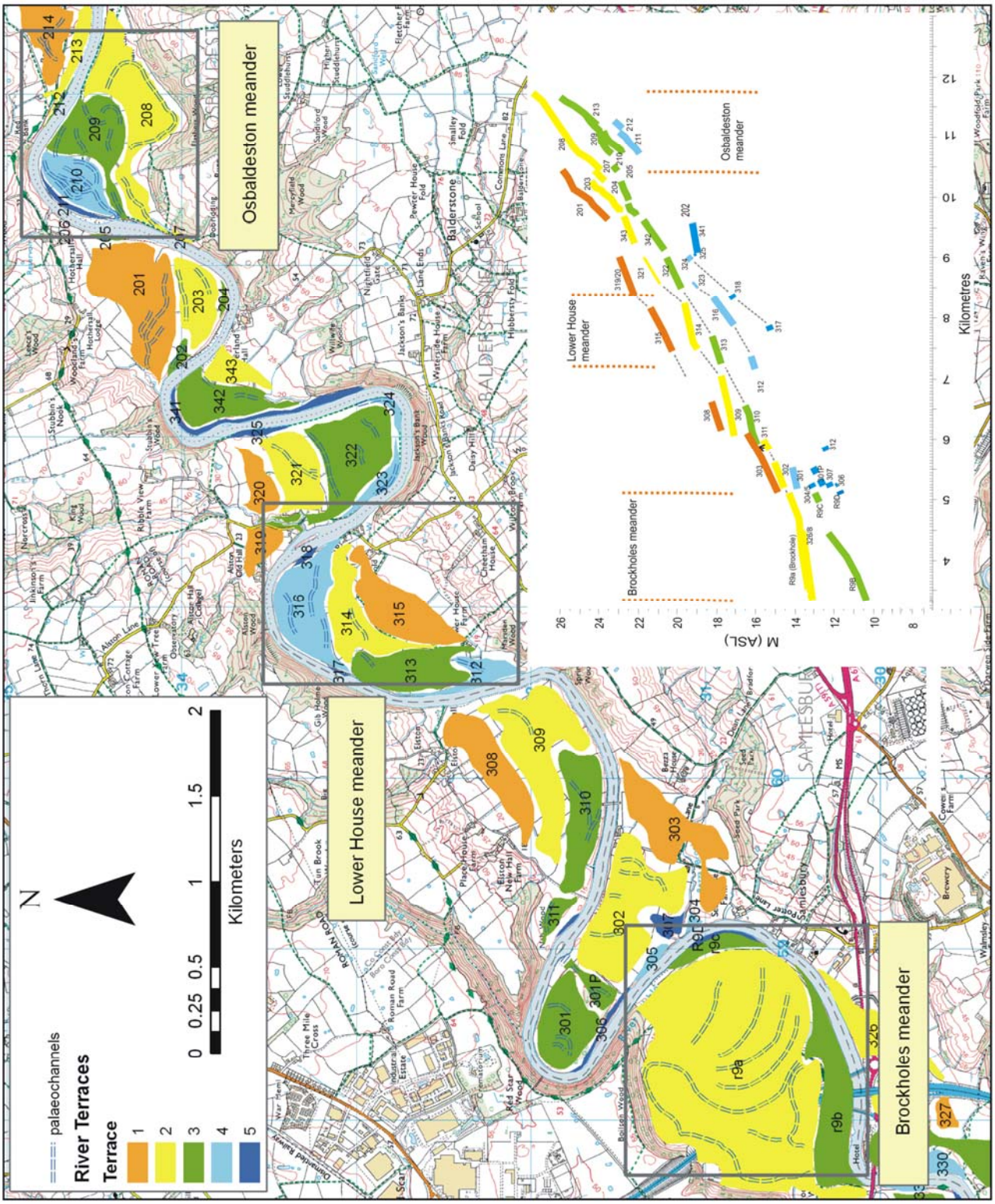

Figure 74: Overview geomorphological map of the Lower Ribble Valley between the M6 motorway and Osbaldeston Hall, showing river terraces and palaeochannels. Box outlines show the extent of the three study reaches: Brockholes, Lower House Farm and Osbaldeston Hall. Inset shows river terrace height/range diagram

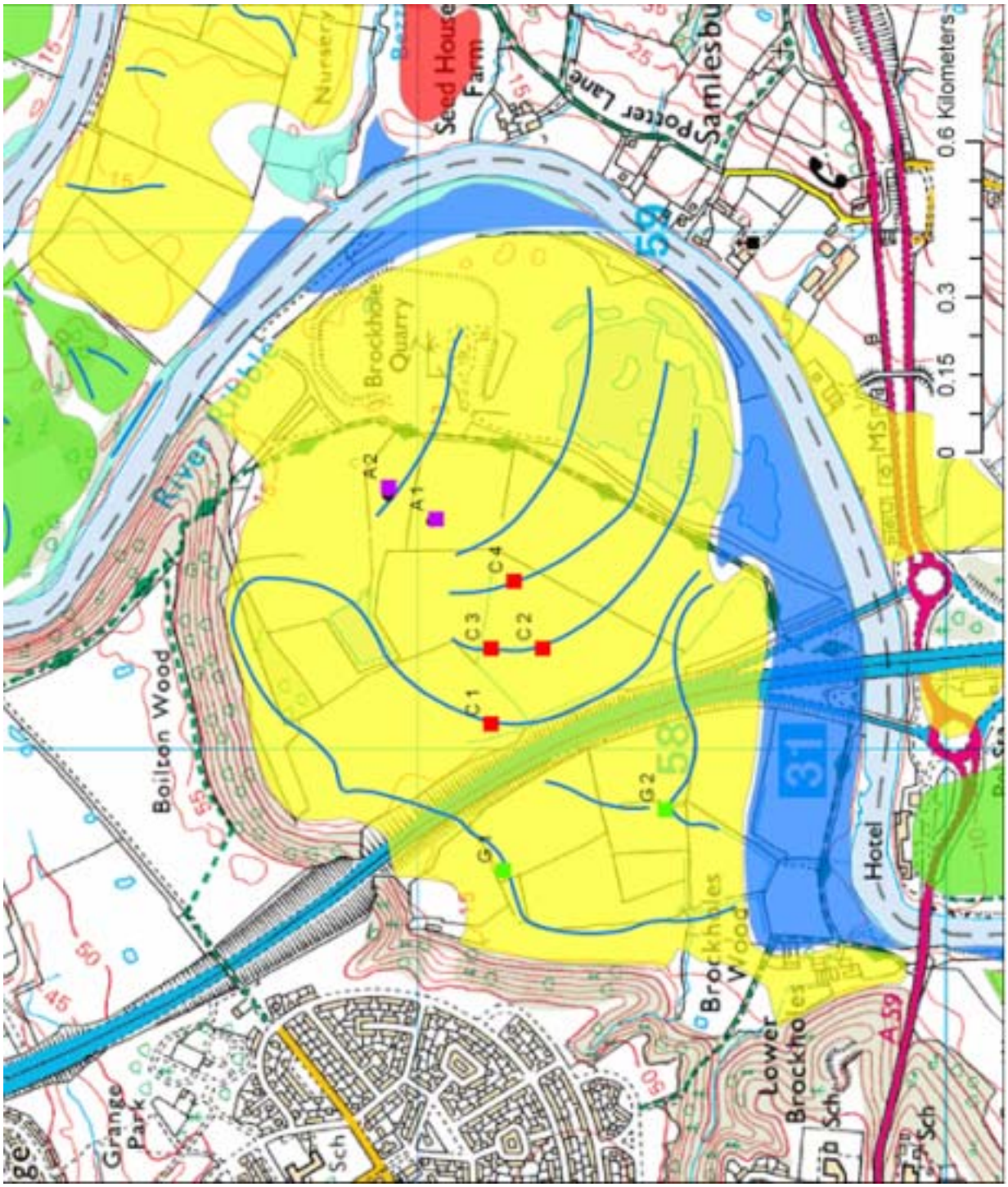

Figure 75: Geomorphological map of the Lower Ribble Valley at Brockholes meander, showing river terraces, palaeochannels and section locations. The key for the river terraces is shown on Figure 74

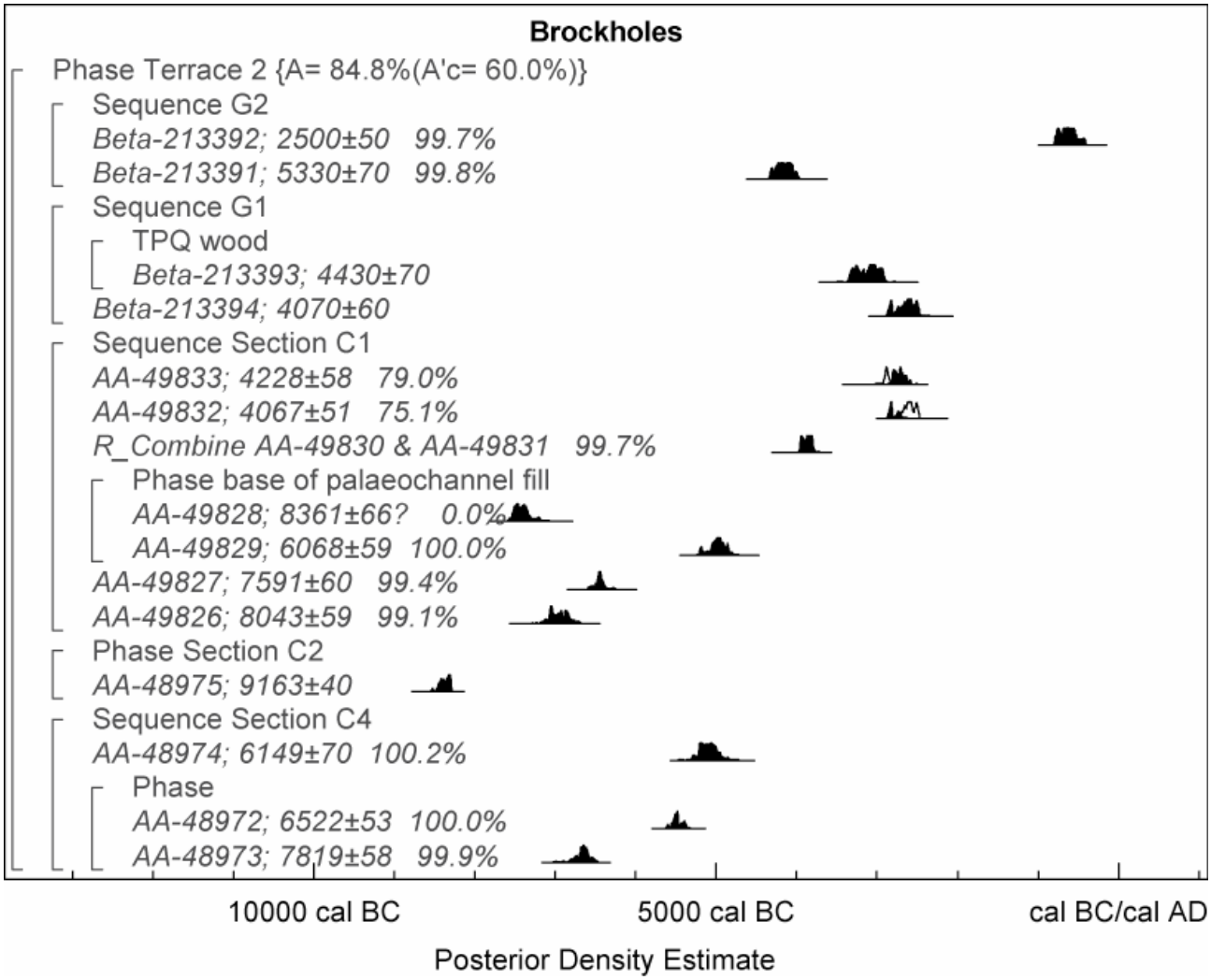

Figure 76: Probability distributions of dates from Brockholes; each distribution represents the relative probability that an event occurs at a particular time. For each of the radiocarbon dates two distributions have been plotted, one in outline, which is the result of simple radiocarbon calibration, and a solid one, which is based on the chronological model used. A question mark (?) indicates that the result has been excluded from the model. The large square brackets on the left, along with the OxCal keywords, define the model exactly

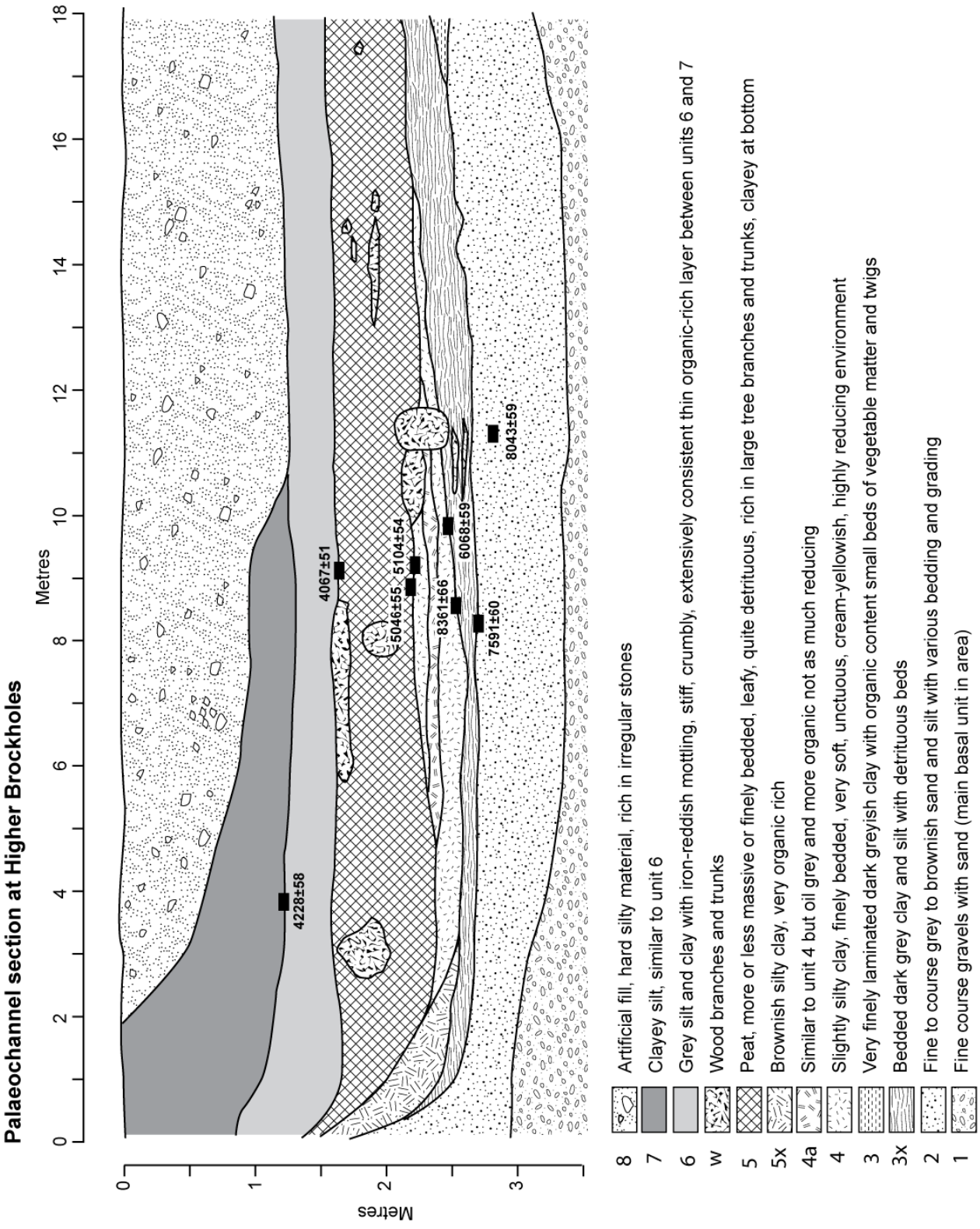

Figure 77: Radiocarbon-dated subsurface sediment sequence (section C1) in the large palaeo-meander loop on terrace T2 at the Brockholes meander recorded by Chiti (2004)

A

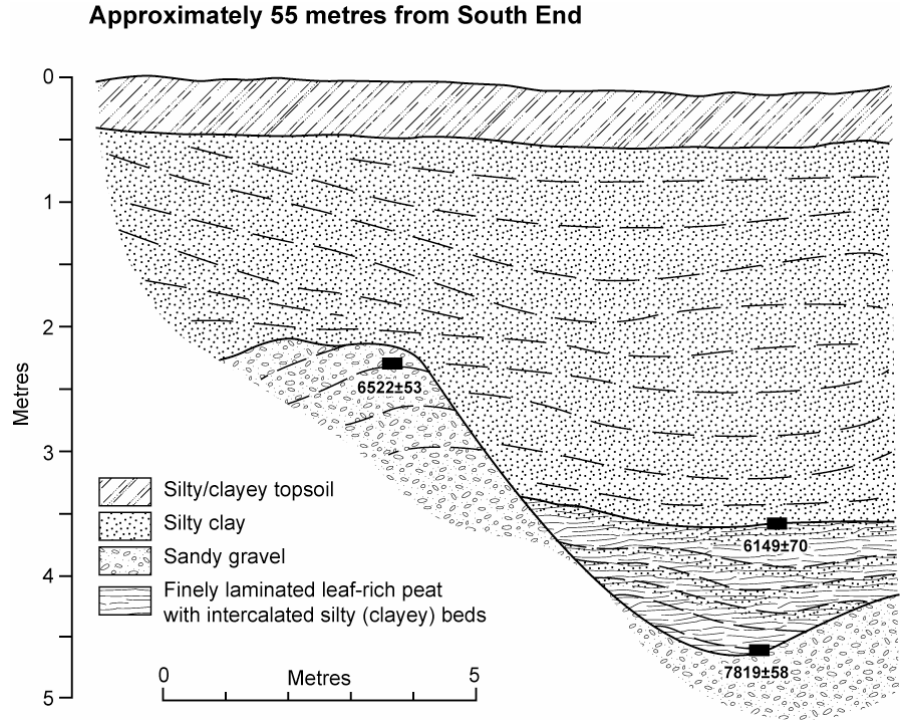

B

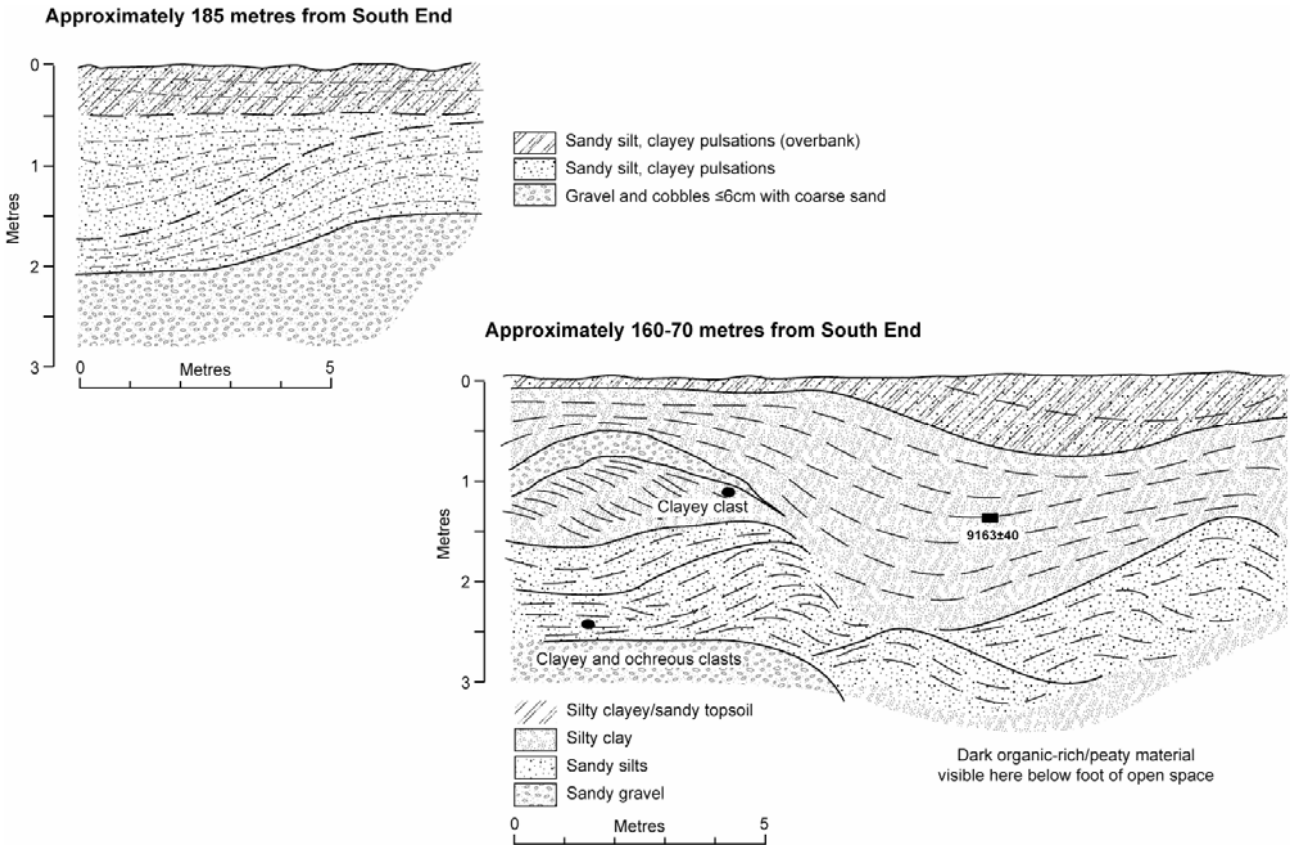

Figure 78: Radiocarbon-dated subsurface sediment sequences from scroll-bar palaeochannels on terrace 2 of the Brockholes meander recorded by Chiti (2004): a) section C4; b) sections C2 and C3

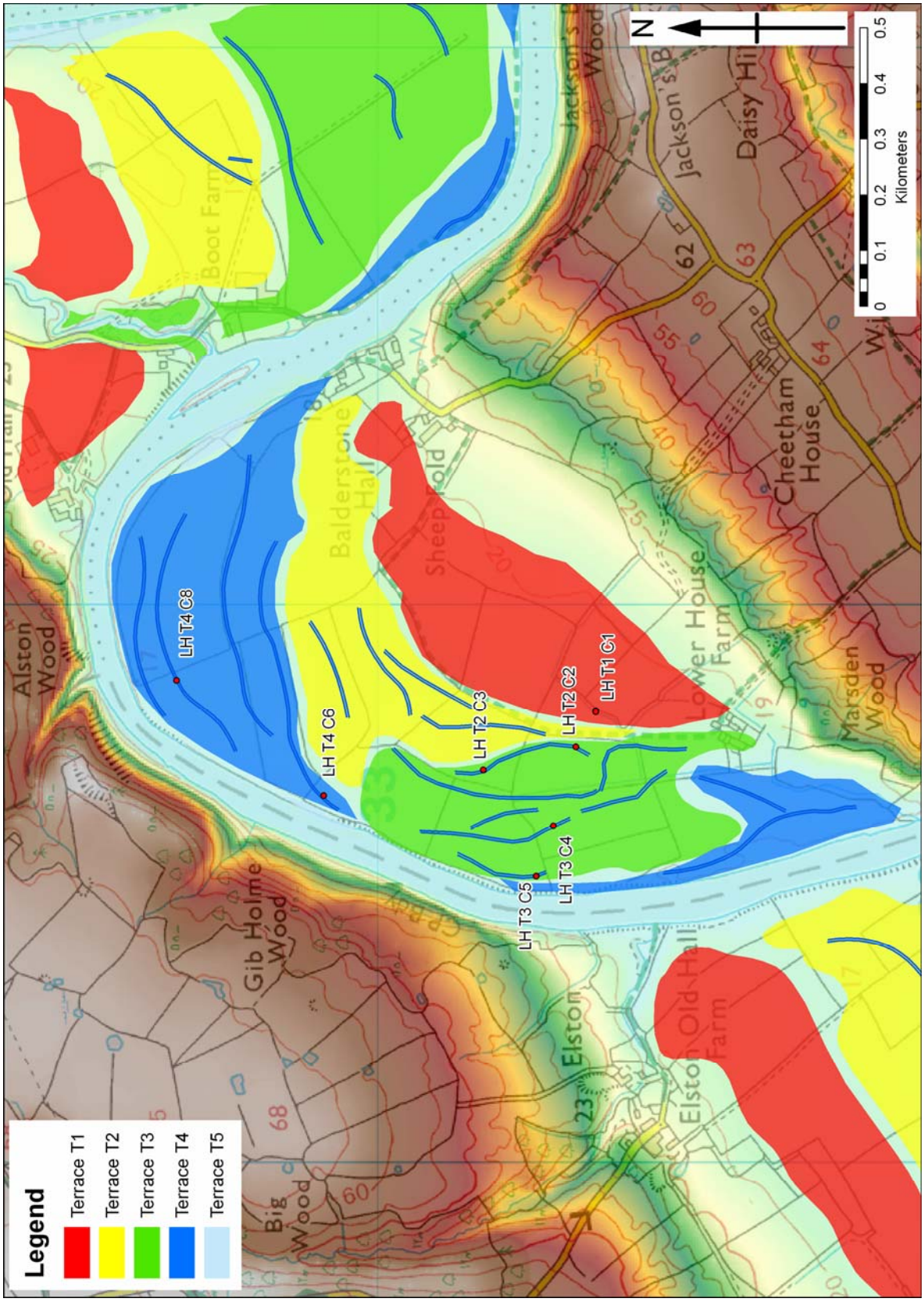

Figure 79: Geomorphological map of the Lower Ribble Valley at the Lower House meander, showing river terraces, palaeochannels and coring location

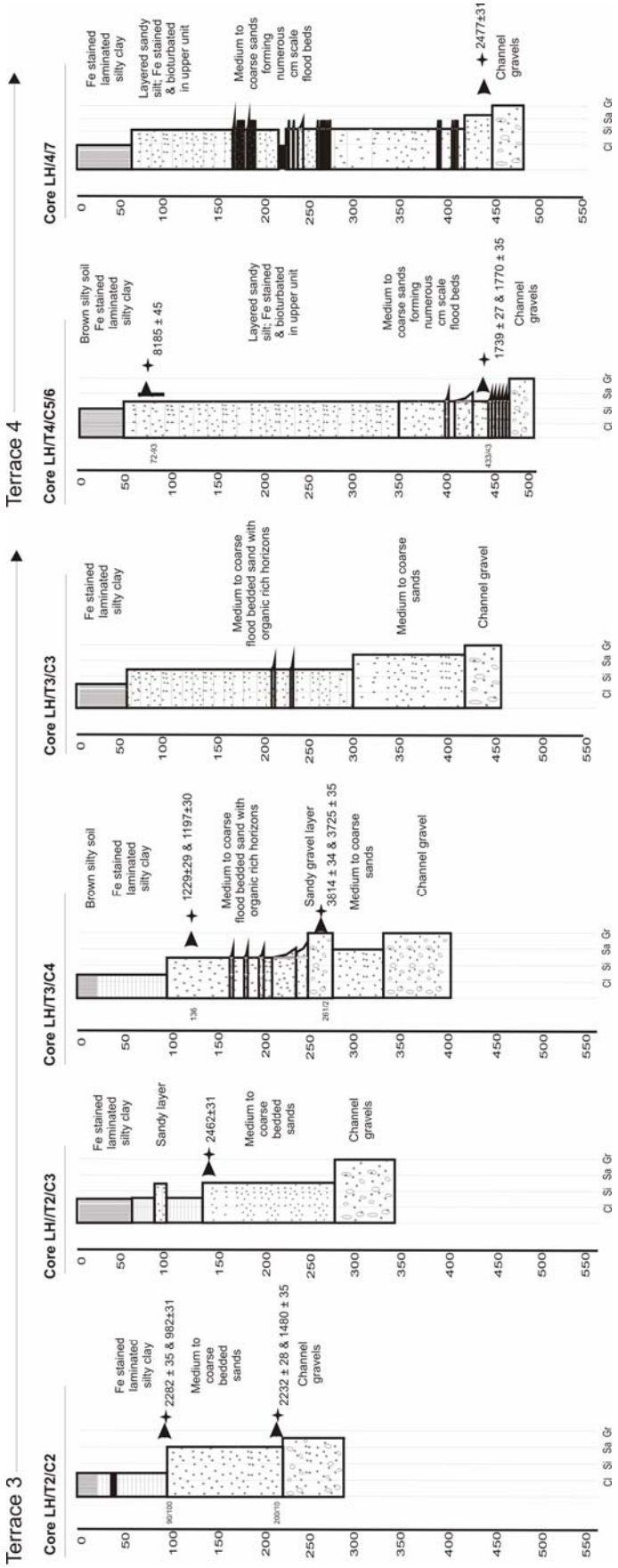

Figure 80: Sediment stratigraphy for boreholes taken at Lower House meander in the Lower Ribble Valley, also showing radiocarbon dates

A.

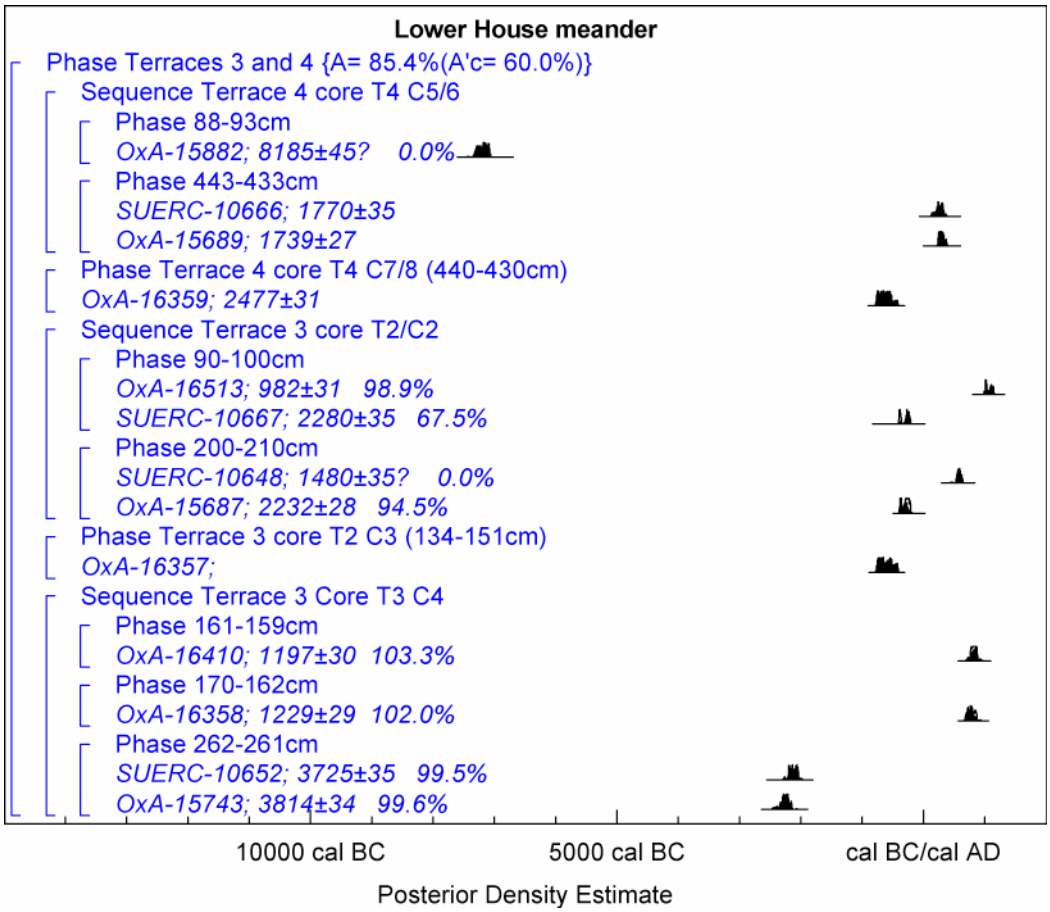

B.

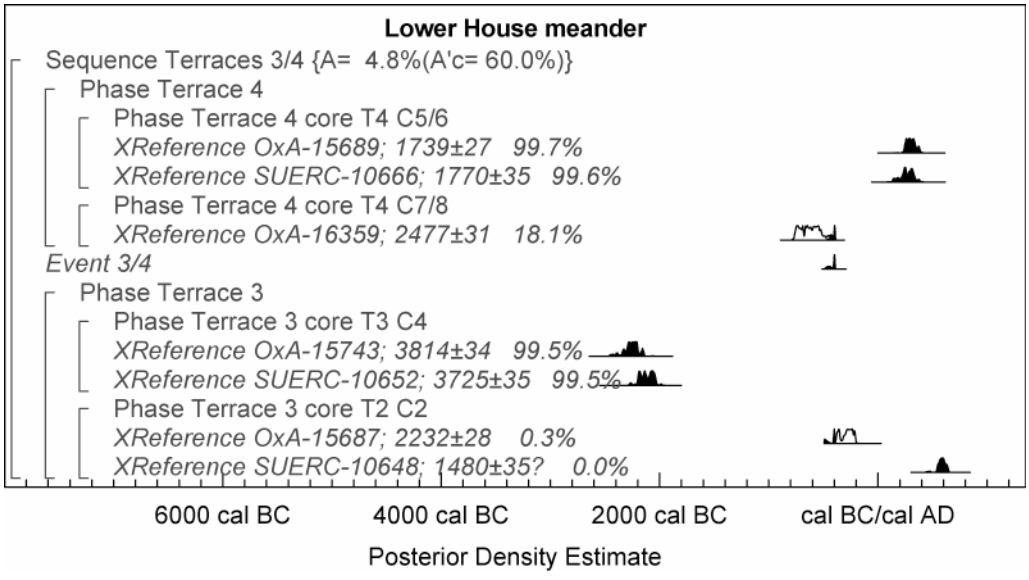

Figure 81:A) Probability distributions of dates from Lower House Farm. Each distribution represents the relative probability that an event occurs at a particular time. For each of the radiocarbon dates two distributions have been plotted, one in outline, which is the result of simple radiocarbon calibration, and a solid one, which is based on the chronological model used. A question mark (*?*) indicates that the result has been excluded from the model. The large square brackets on the left along with the OxCal keywords define the model. B) Chronology of Lower House Farm terraces 3 and 4. The results are included in a Bayesian model, whose format is identical to that of Part A. Distributions labelled *XReference* have been imported from the model in Part A. The other distributions correspond to aspects of the model. For example, the distribution '*Event 3/4*' is the estimated date for the switch from T3 to T4

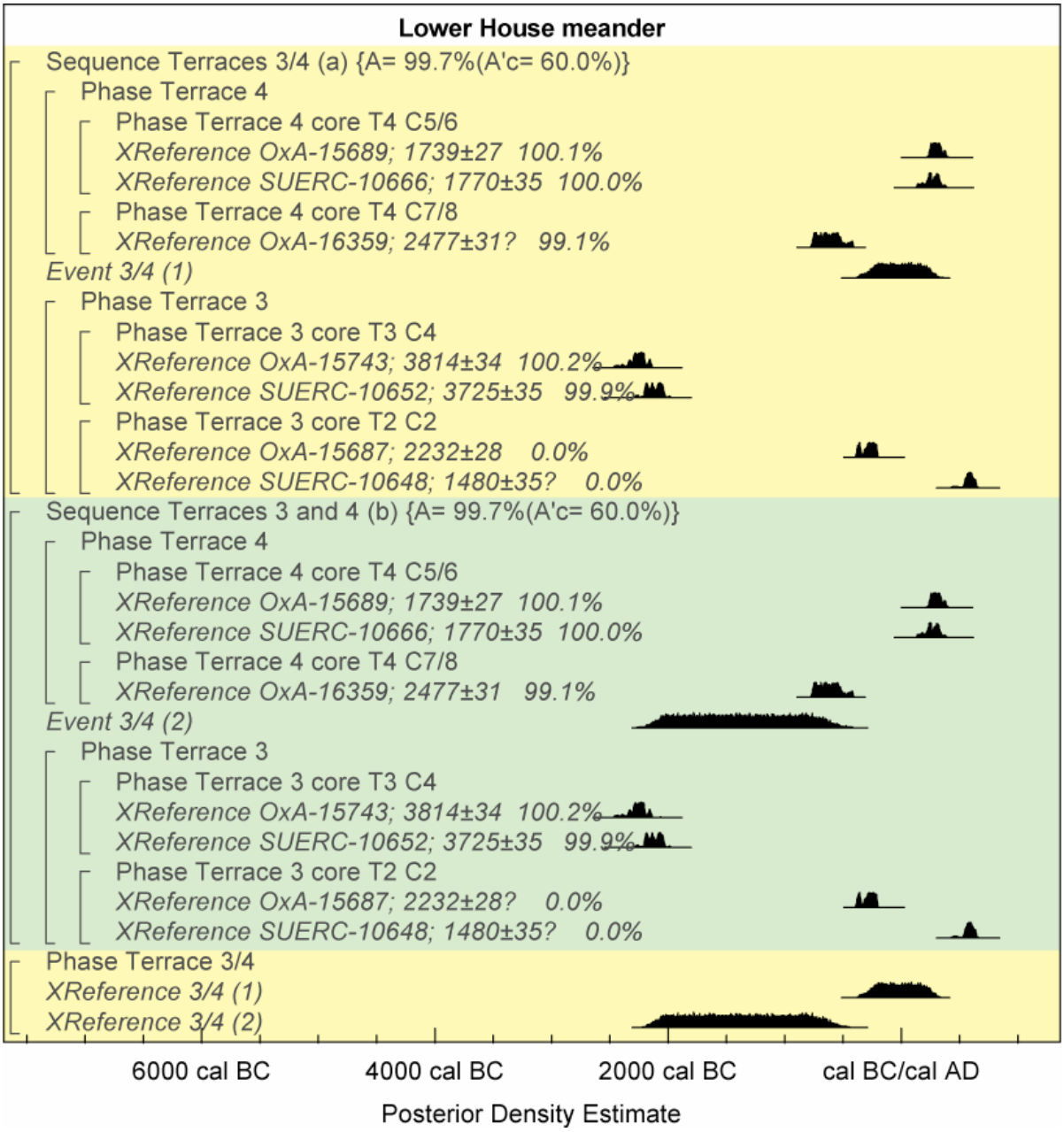

Figure 82: Chronology of Lower House Farm terraces T3 and T4. The results are included in a model, whose format is identical to that of Figure 81. Distributions labelled *XReference* have been imported from the model in Figure 81. The other distributions correspond to aspects of the model. For example, the distribution '*Event 3/4*' is the estimated date for the switch from T3 to T4. A question mark (*?*) indicates that the result has been excluded from the model

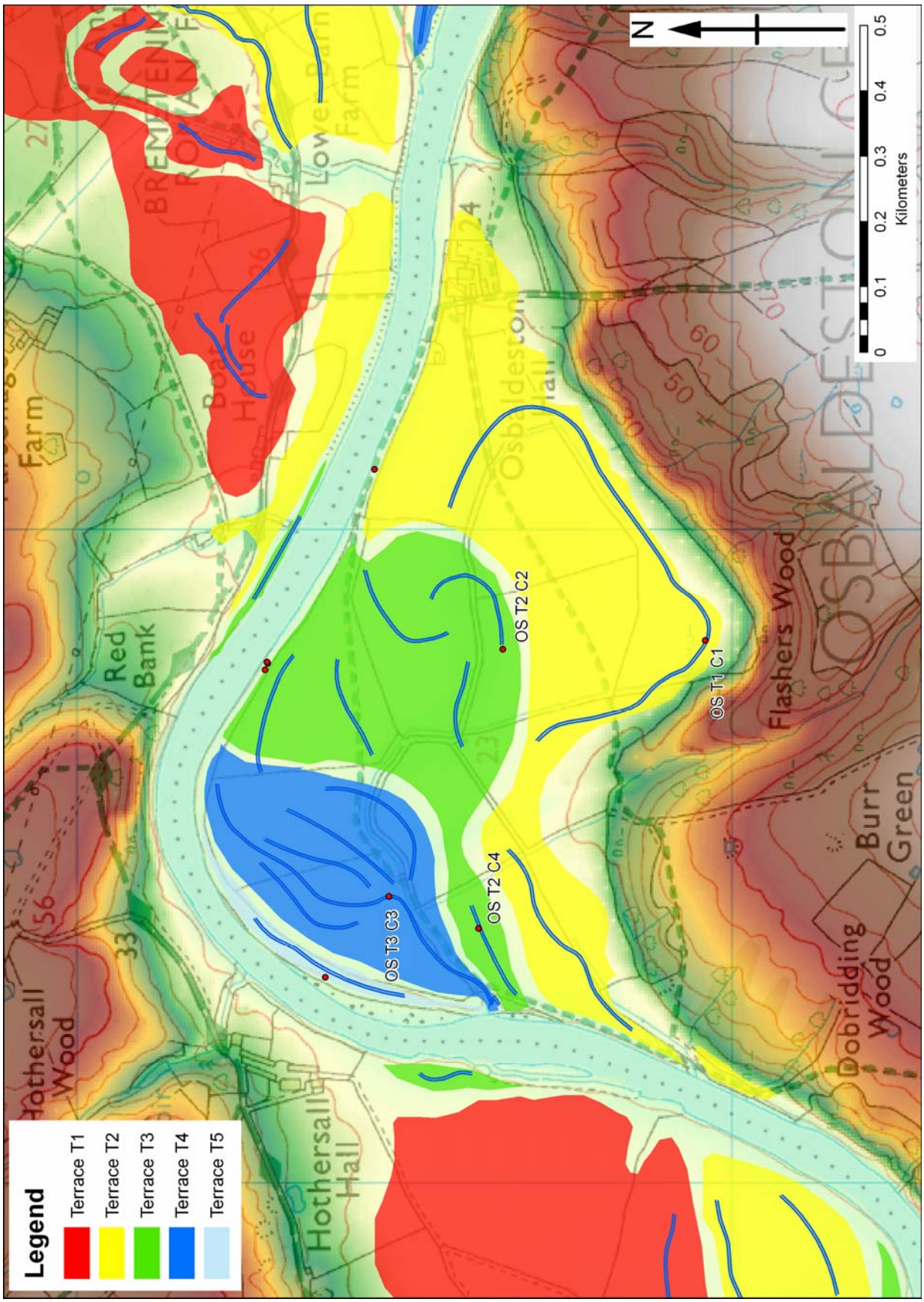

Figure 83: Geomorphological map of the Osbaldeston meander in the Lower Ribble Valley, showing river terraces, palaeochannels and core/bank section locations

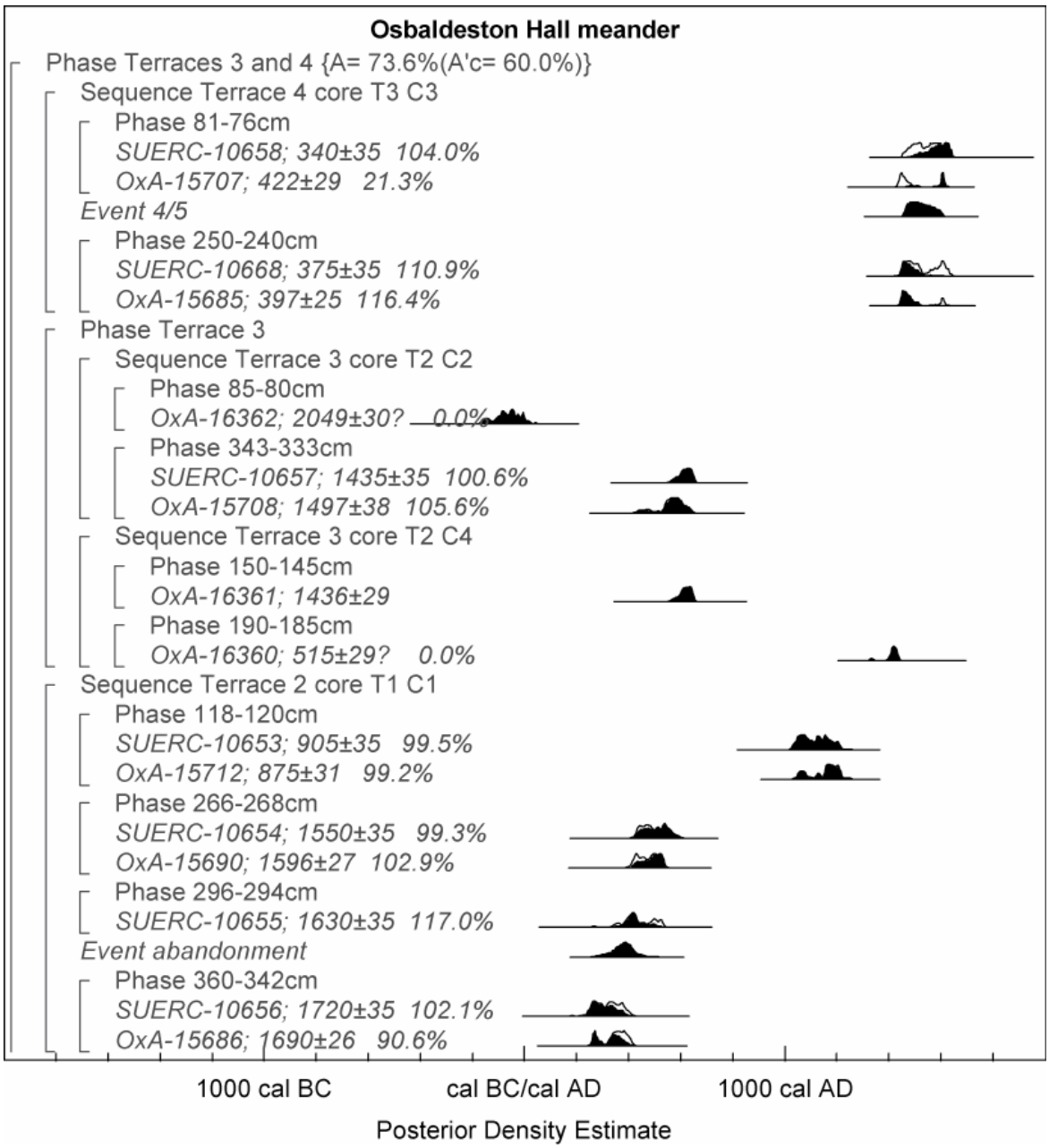

Figure 84: Probability distributions of dates from Osbaldeston Hall. Each distribution represents the relative probability that an event occurs at a particular time. For each of the radiocarbon dates two distributions have been plotted: the outline is the result of simple radiocarbon calibration, and the solid is based on the chronological model used. The other distributions correspond to aspects of the model. For example, the distribution '*Event abandonment*' is the estimated date for the abandonment of terrace T2. A question mark (*?*) indicates that the result has been excluded from the model. The large square brackets on the left, along with the OxCal keywords, define the model exactly

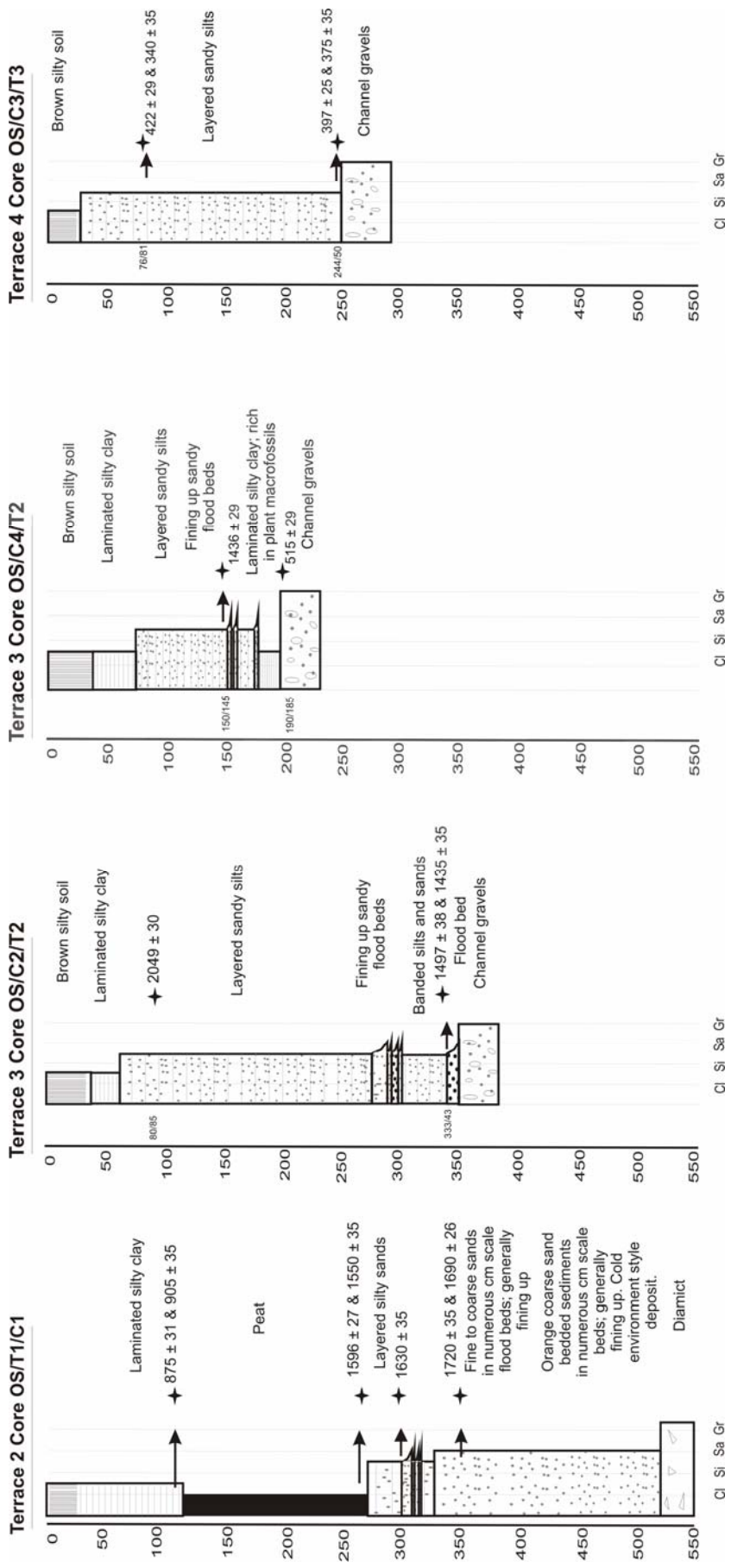

Figure 85: Sediment stratigraphy for boreholes taken at Osbaldeston Hall meander in the Lower Ribble Valley, also showing radiocarbon dates

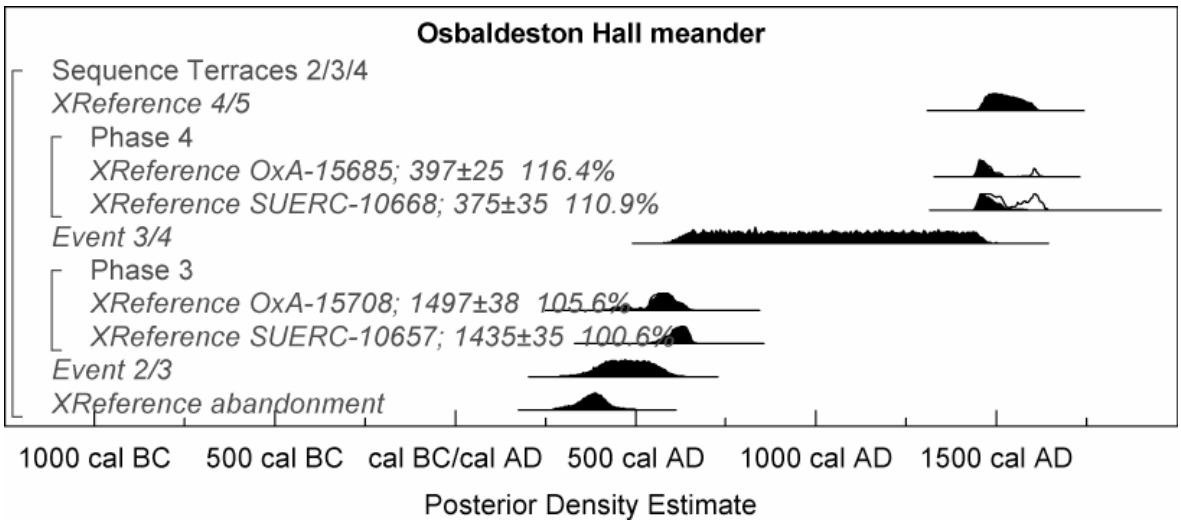

Figure 86: Chronology of Osbaldeston Hall terraces T3 and T4. The results are included in a model, whose format is identical to that of Figure 85. Distributions labelled *XReference* have been imported from the model in Figure 85. The other distributions correspond to aspects of the model. For example, the distribution '*Event 3/4*' is the estimated date for the switch from T3 to T4

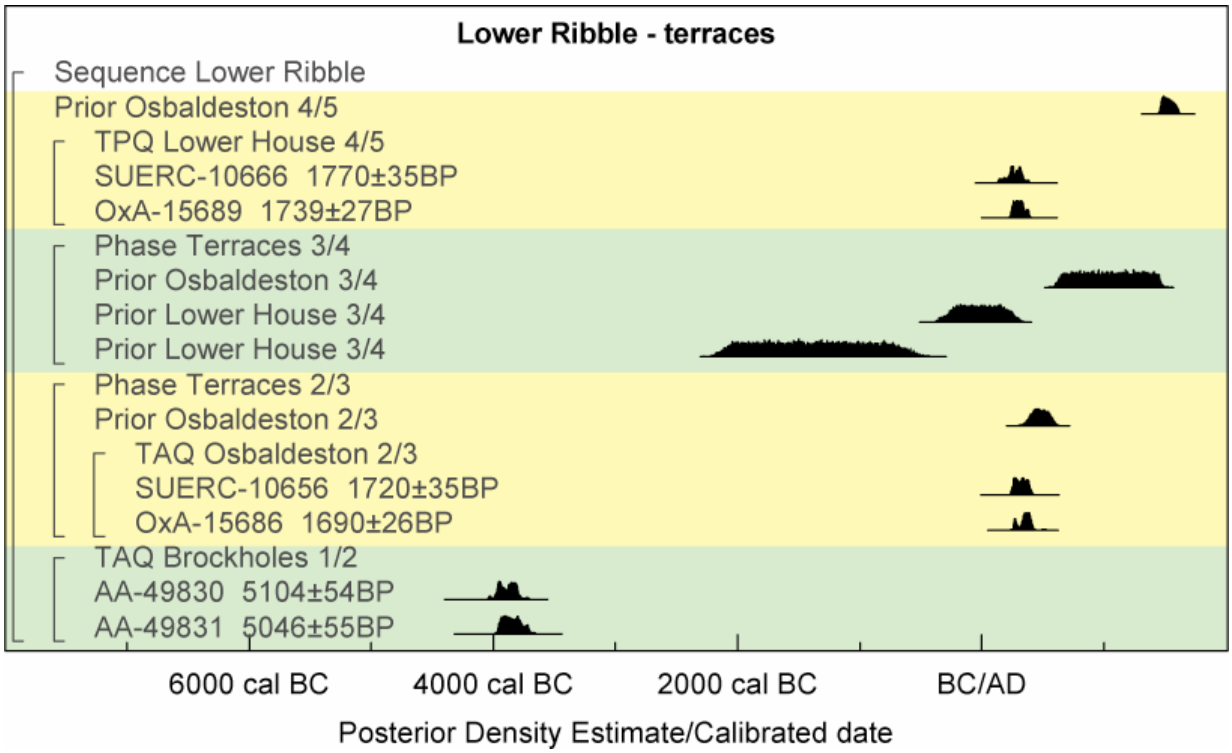

Figure 87: Chronological summaries for the main dated terrace events in the Lower Ribble Valley. Distributions labelled *Prior* have been imported from the models in Figures 81B and 84

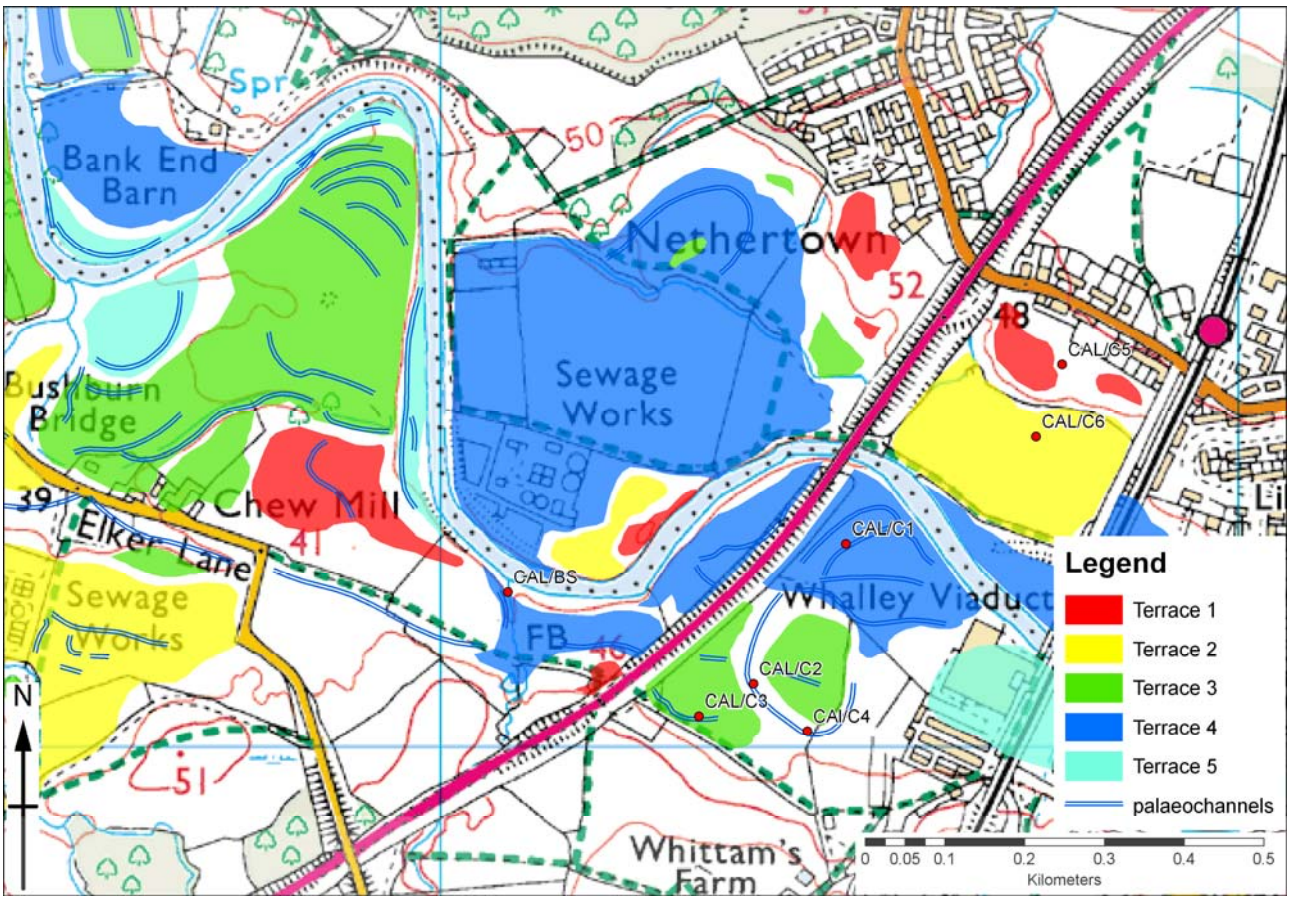

Figure 88: Geomorphological map of the Lower Calder at Whalley, showing river terraces, palaeochannels and the location of coring sites and bank sections

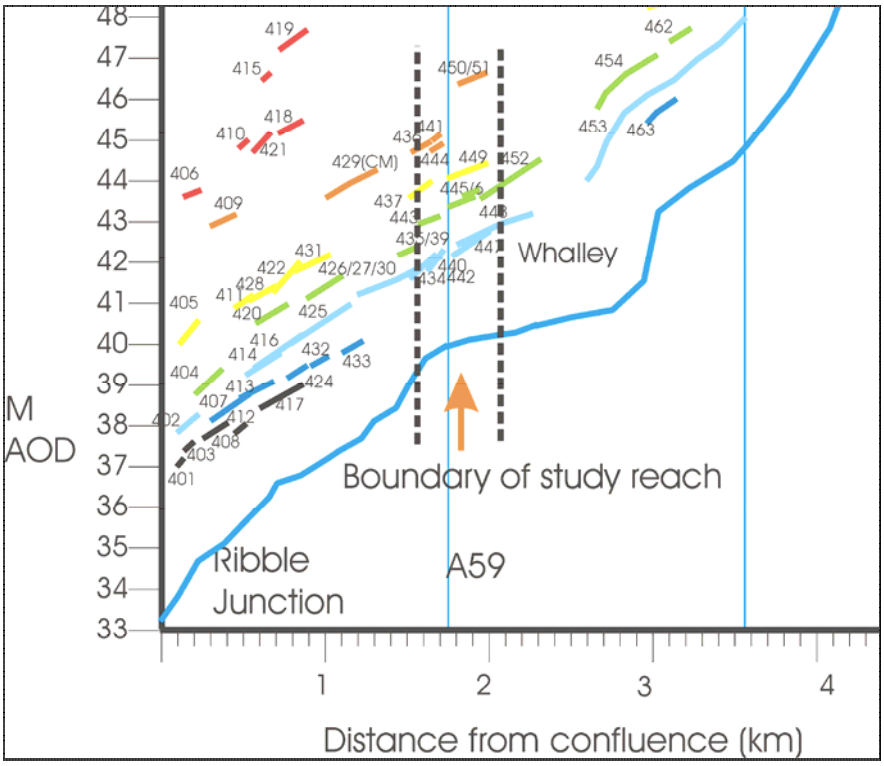

Figure 89: LiDAR-derived height range diagram for the Lower Calder

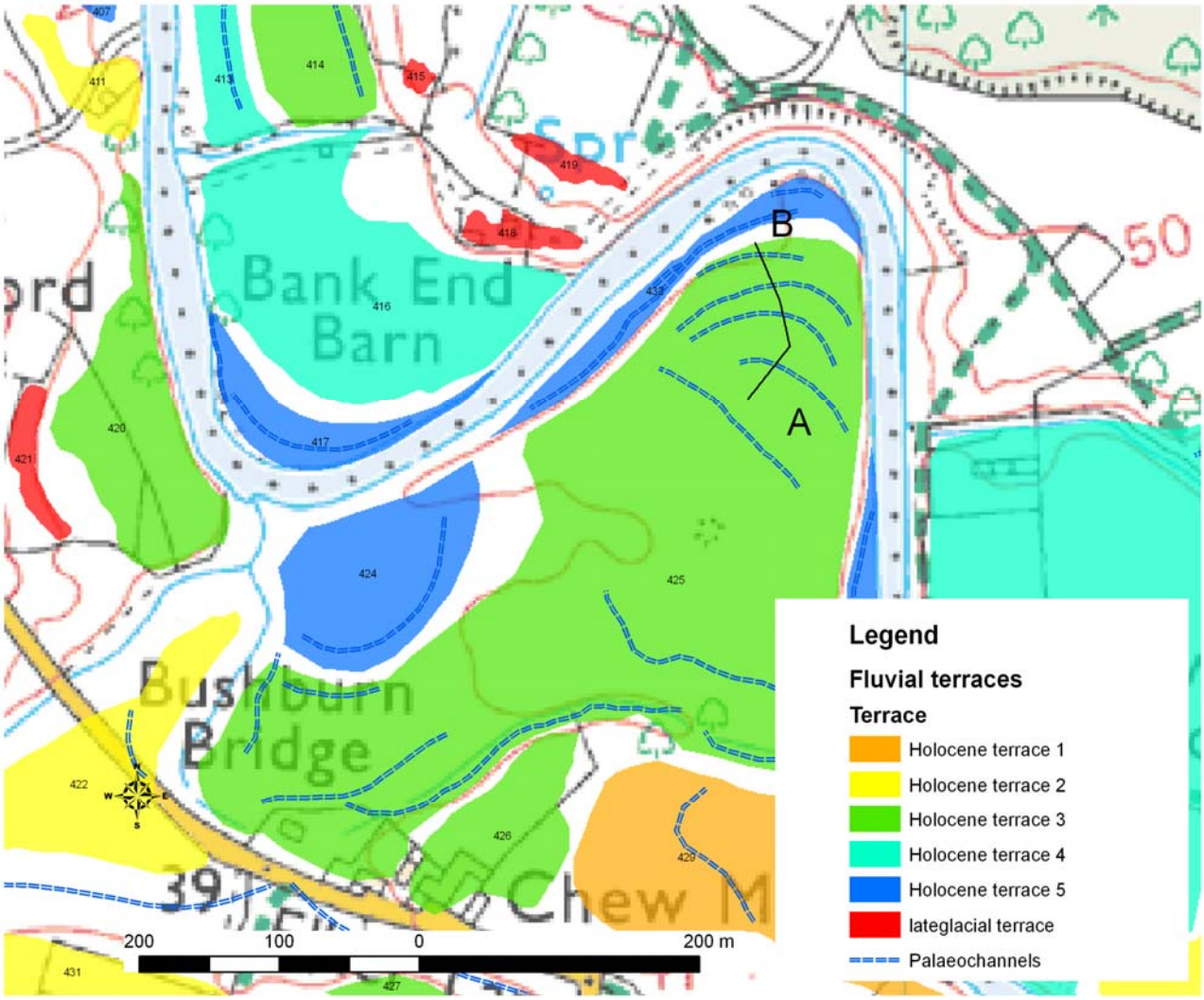

Figure 90: Example of lateral channel changes on Lower Calder river terrace T3

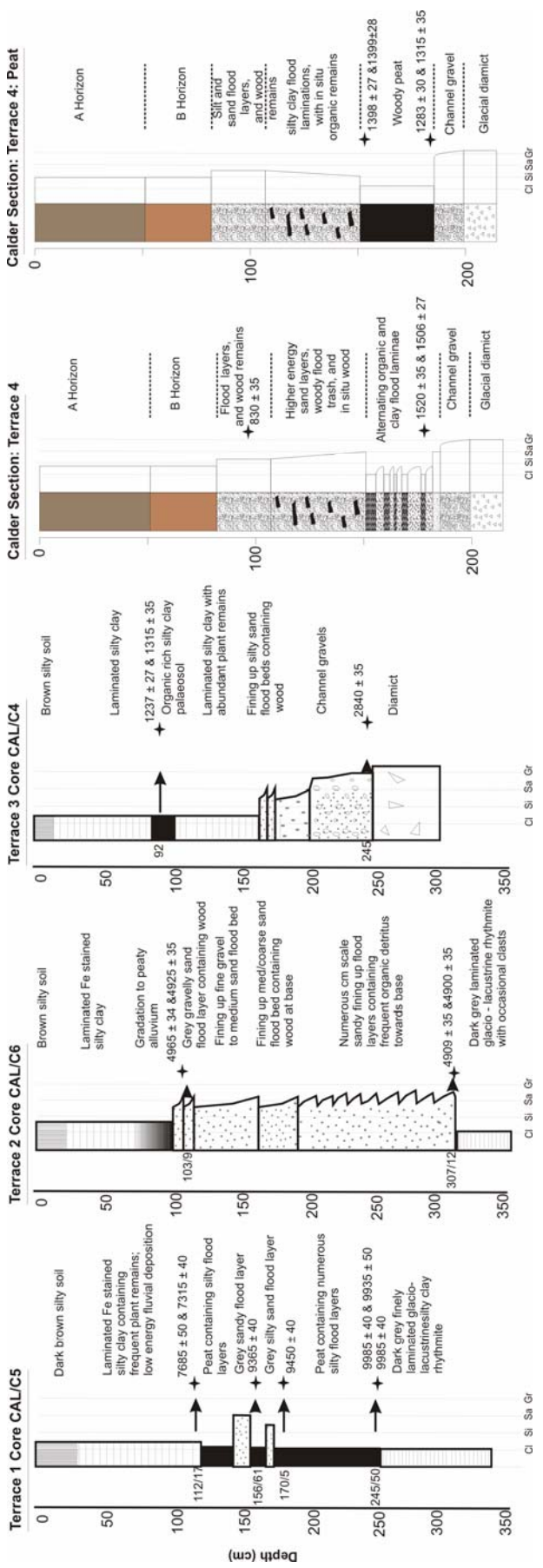

Figure 91: Sediment stratigraphy for boreholes taken at Whalley in the Lower Calder Valley, also showing radiocarbon dates

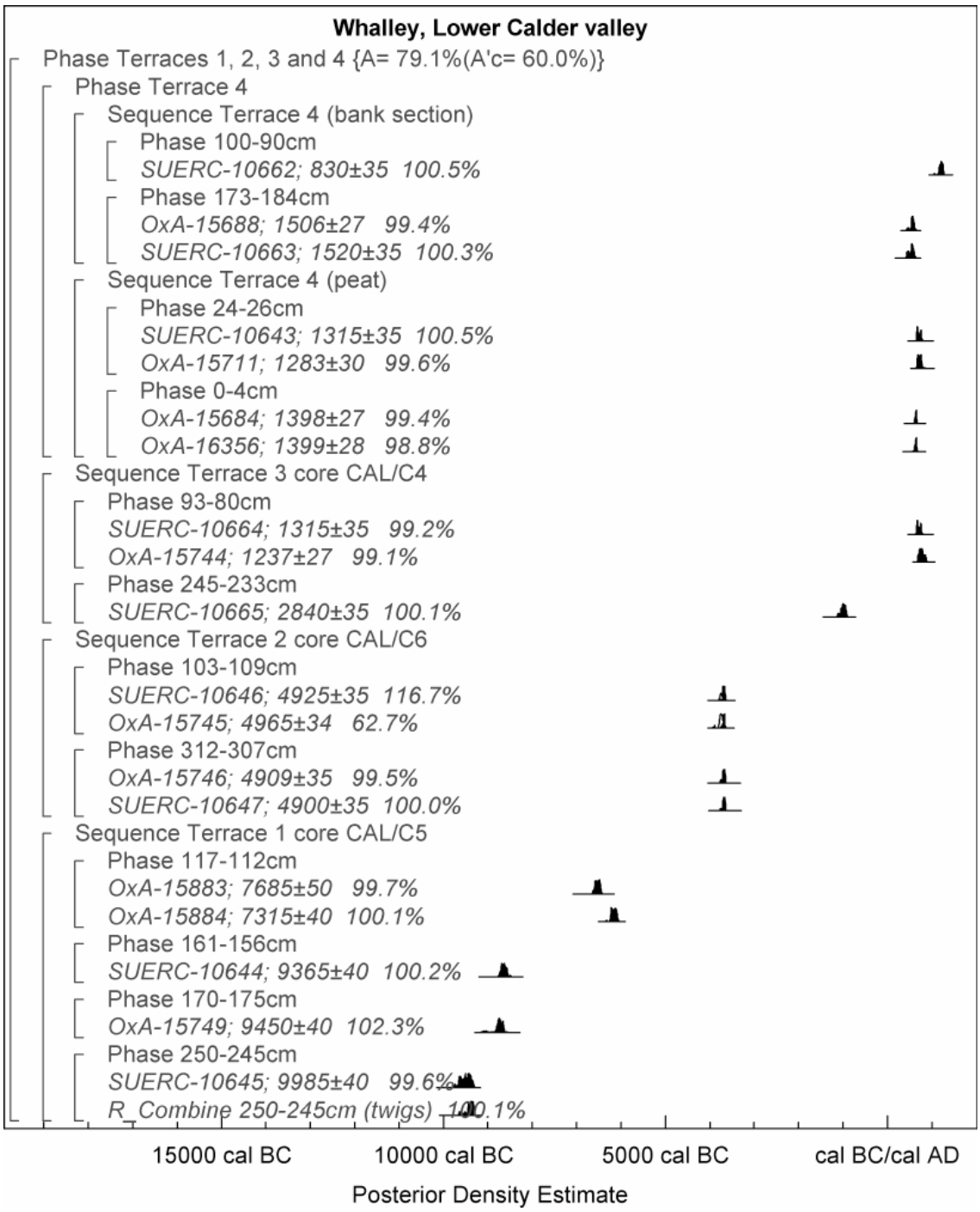

Figure 92: Probability distributions of dates from Whalley, Lower Calder Valley. Each distribution represents the relative probability that an event occurs at a particular time. For each of the radiocarbon dates two distributions have been plotted, one in outline, which is the result of simple radiocarbon calibration, and a solid one, which is based on the chronological model used. The large square brackets down the left hand side along with the OxCal keywords define the model exactly

Figure 93: Looking east along river bank exposures that show basal diamicton, fluvial channel and bar-form gravels overlain by a 500 mm thick peat-bed and then overbank alluvium. The deposits are from terrace T4 of the lower Calder, near Whalley. The right hand end of the photograph shows the peat-filled back channel, whereas exposures of flood laminated organic-rich alluvial channel fill characterizes the left end of the section, which is from the centre of a palaeochannel

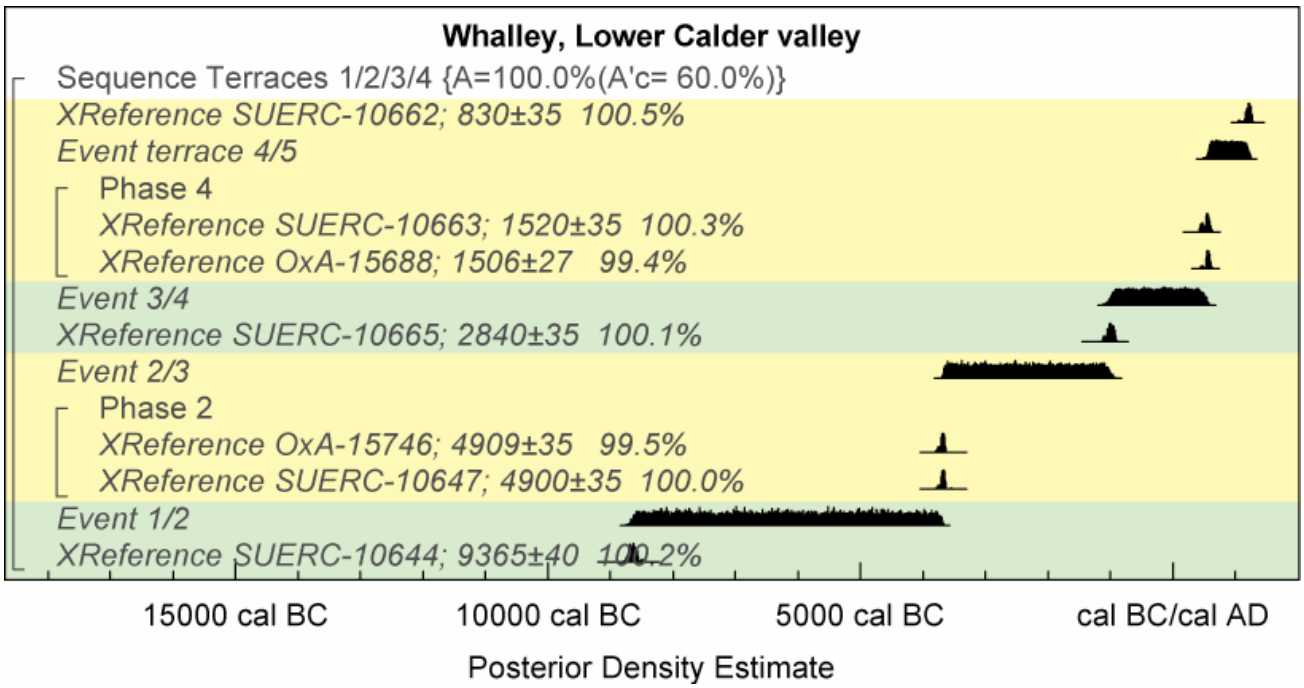

Figure 94: Chronology of Whalley, Lower Calder Valley terraces T1, T2, T3 and T4. The results are included in a model, whose format is identical to that of Figure 92. Distributions labelled *XReference* have been imported from the model in Figure 92. The other distributions correspond to aspects of the model. For example, the distribution '*Event 3/4*' is the estimated date for the switch from T3 to T4

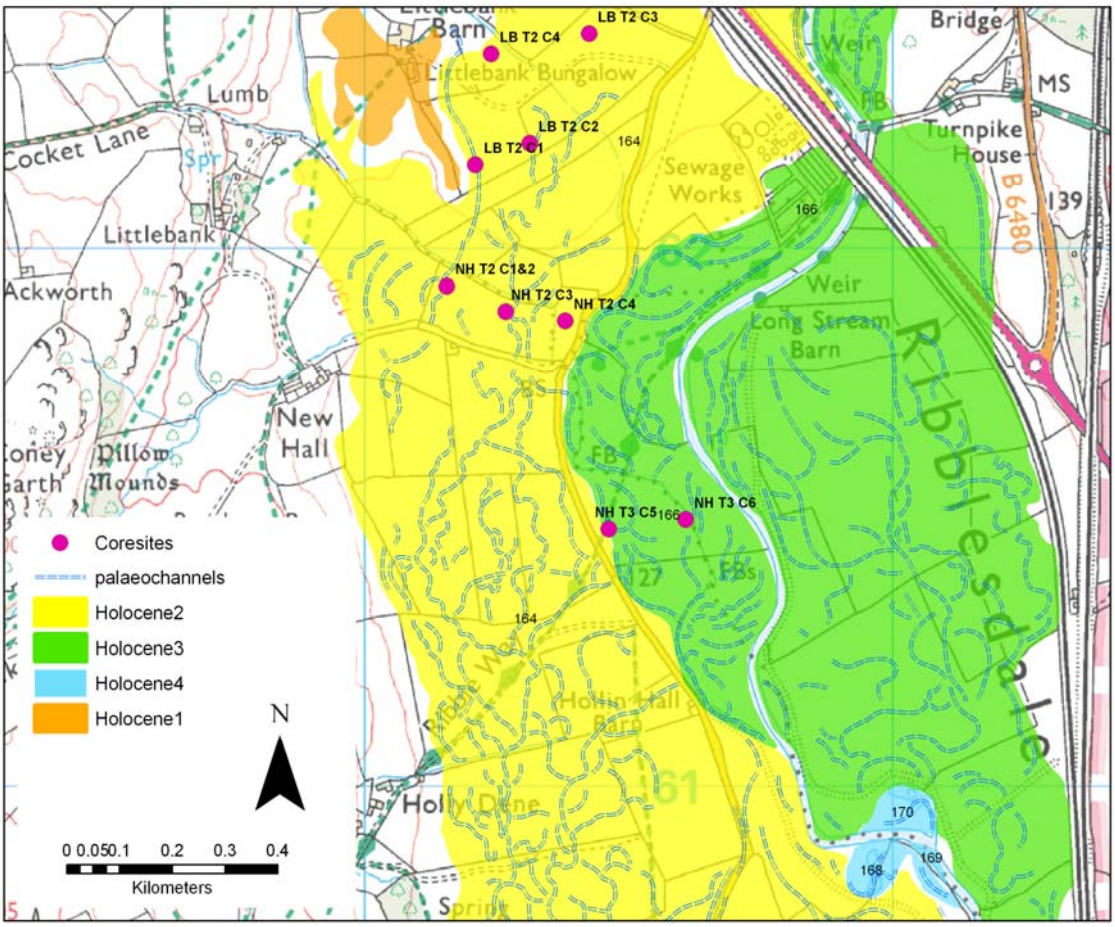

Figure 95: Geomorphological map of the Upper Ribble Valley ‘flood basin’, showing river terraces, palaeochannels and coring locations

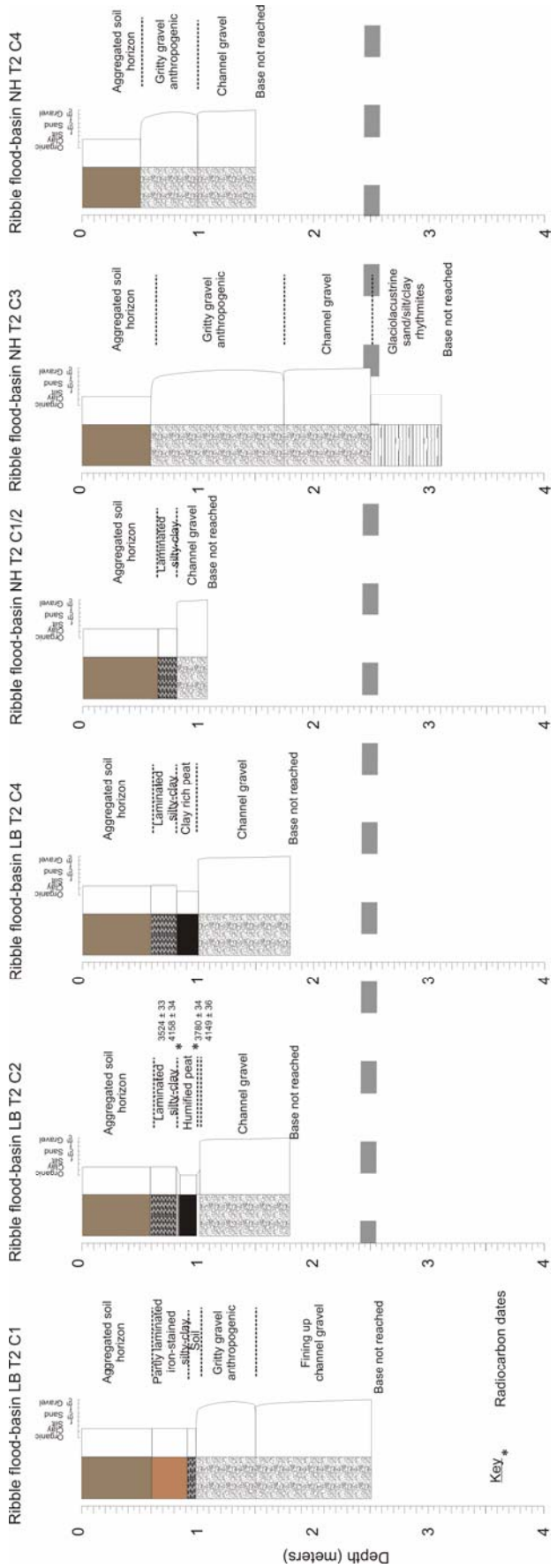

Figure 96: Sediment stratigraphy for terrace T2 in the Upper Ribble 'flood basin' at Littlebank and New House Farms, also showing the radiocarbon dates

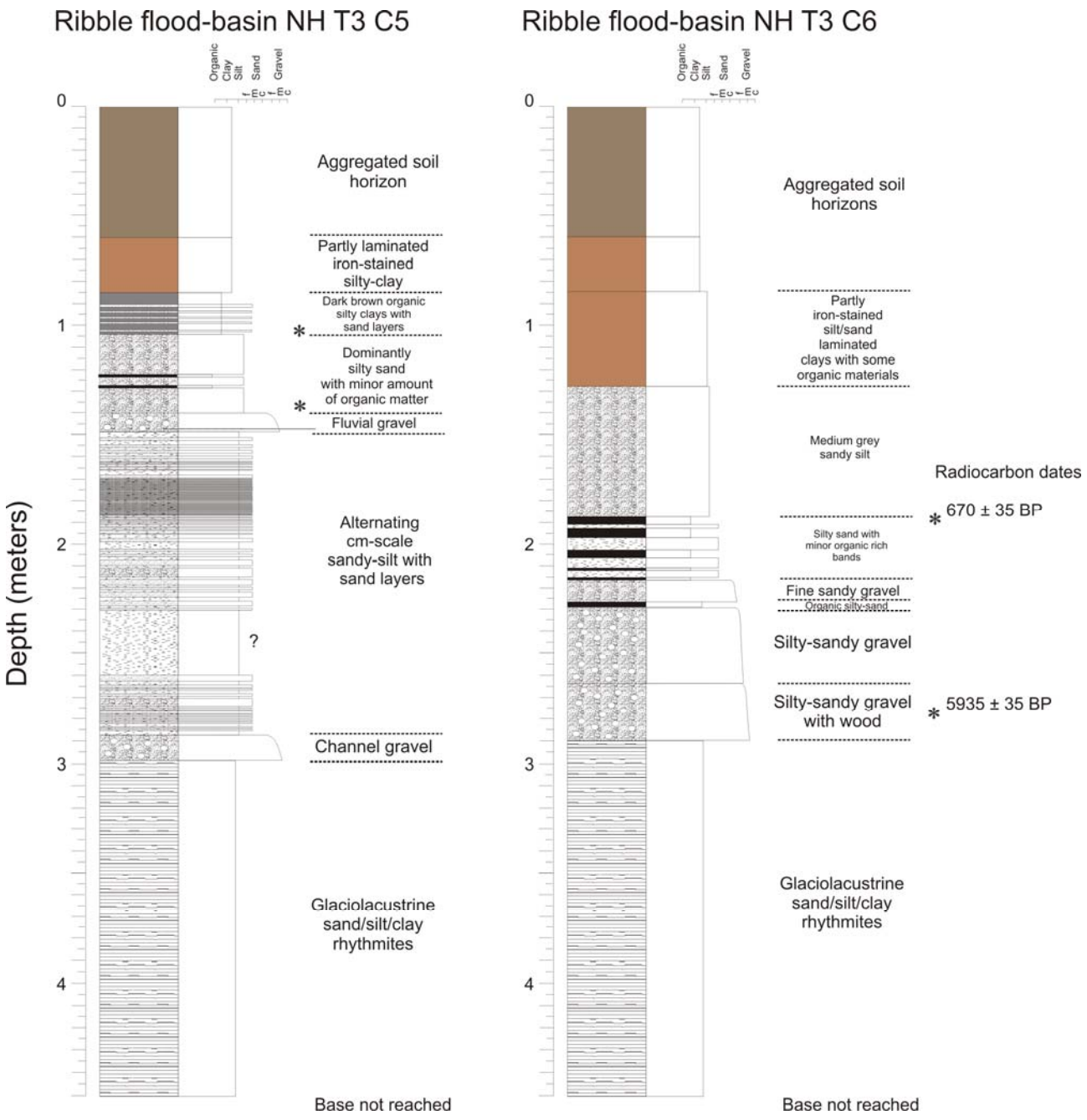

Figure 97: Sediment stratigraphy for terrace T3 in the Upper Ribble ‘flood basin’ at New House Farm, also showing the radiocarbon dates

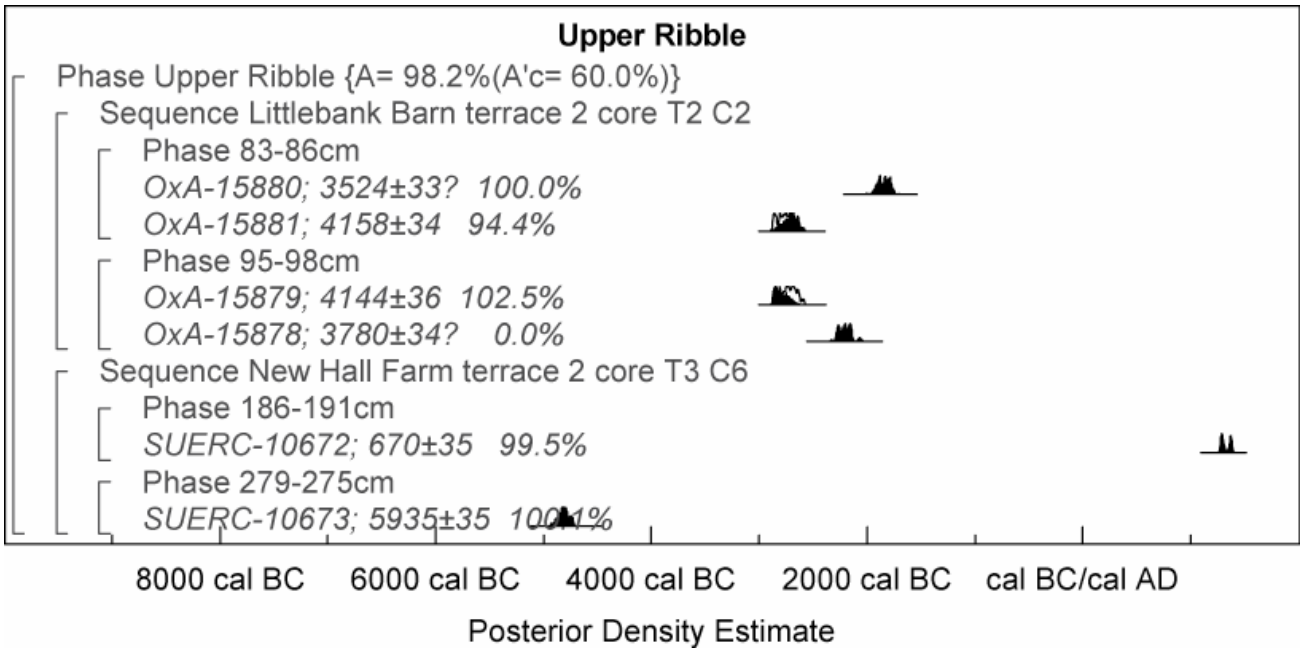

Figure 98: Probability distributions of dates from the Upper Ribble Valley. Each distribution represents the relative probability that an event occurs at a particular time. For each of the radiocarbon dates two distributions have been plotted, one in outline, which is the result of simple radiocarbon calibration, and a solid one, which is based on the chronological model used. A question mark (*?*) indicates that the result has been excluded from the model. The large square brackets on the left, along with the OxCal keywords, define the model exactly

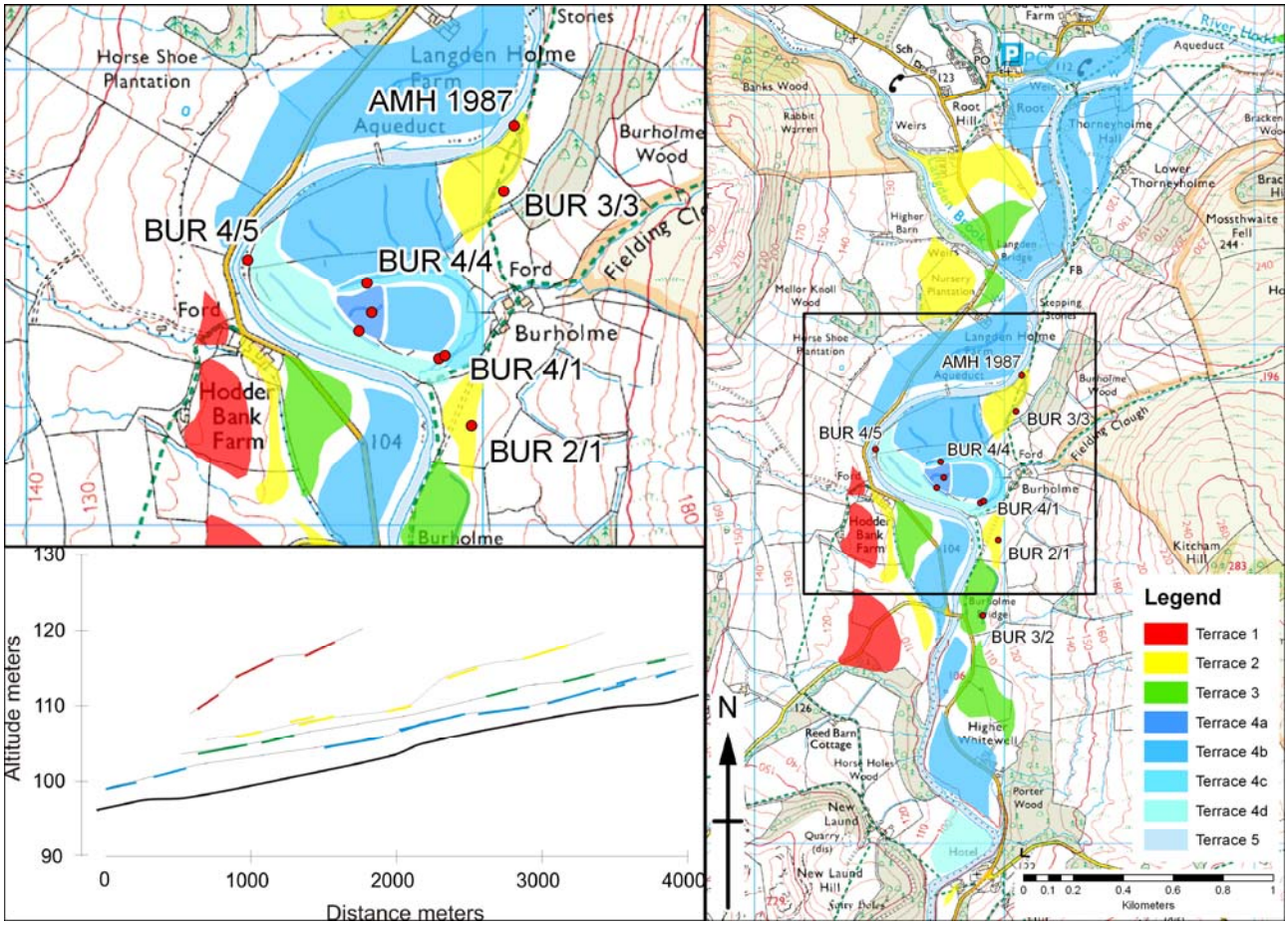

Figure 99: Geomorphological map of the Hodder Valley at Burholme, showing river terraces, palaeochannels and coring locations

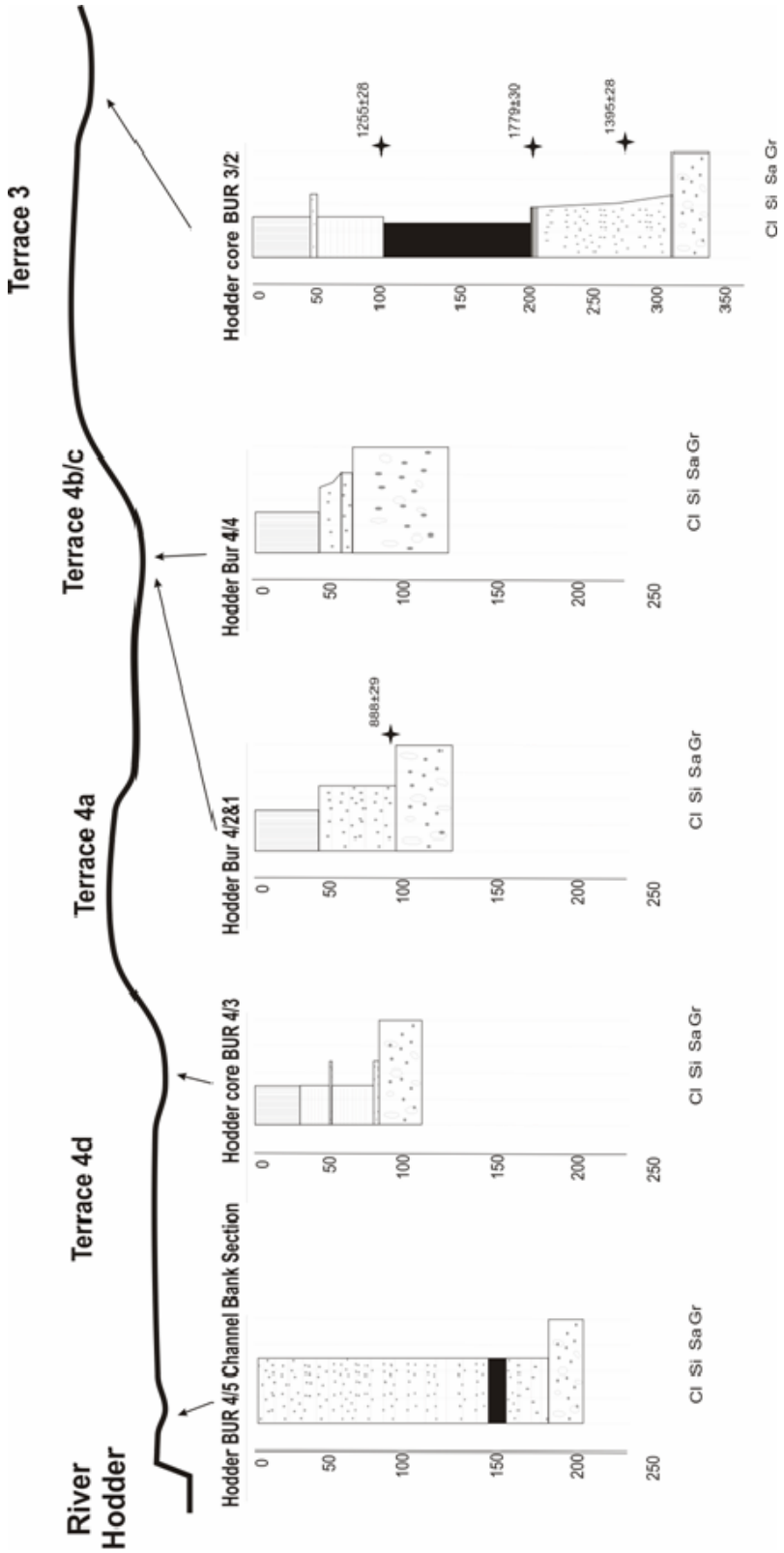

Figure 100: Subsurface sediment stratigraphy in the Hodder Valley at Burholme, showing the position of radiocarbon dates

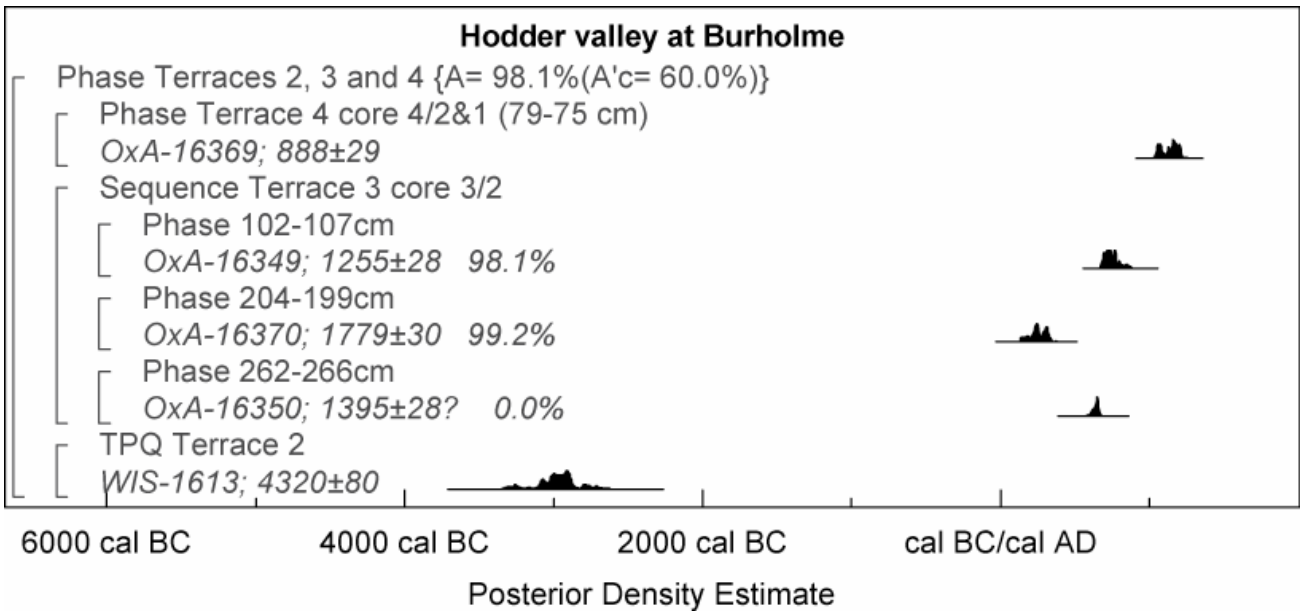

Figure 101: Probability distributions of dates from the Hodder Valley. Each distribution represents the relative probability that an event occurs at a particular time. For each of the radiocarbon dates two distributions have been plotted, one in outline, which is the result of simple radiocarbon calibration, and a solid one, which is based on the chronological model used. A question mark (*?*) indicates that the result has been excluded from the model. The large square on the left, along with the OxCal keywords, define the model exactly

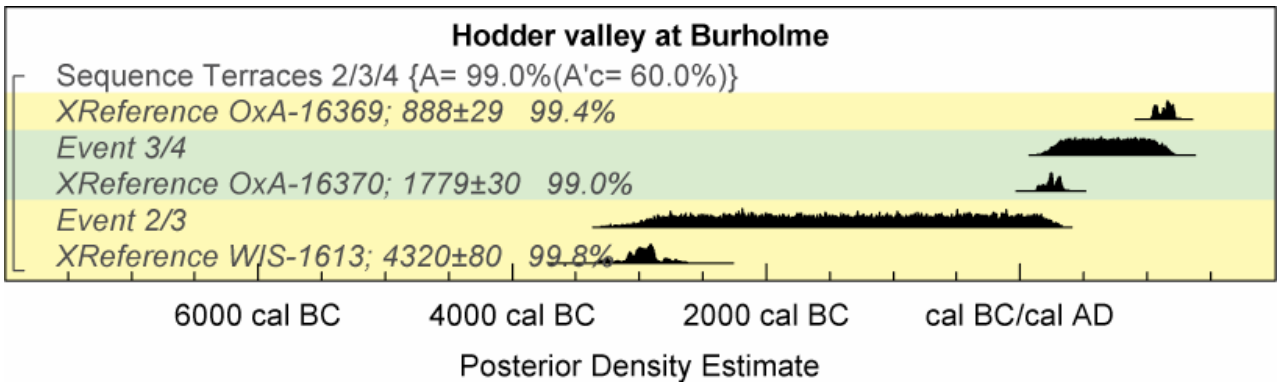

Figure 102: Chronology of Hodder Valley terraces T2, T3 and T4. The results are included in a model, whose format is identical to that of Figure 101. Distributions labelled *XReference* have been imported from the model in Figure 101. The other distributions correspond to aspects of the model. For example, the distribution '*Event 3/4*' is the estimated date for the switch from T3 to T4.

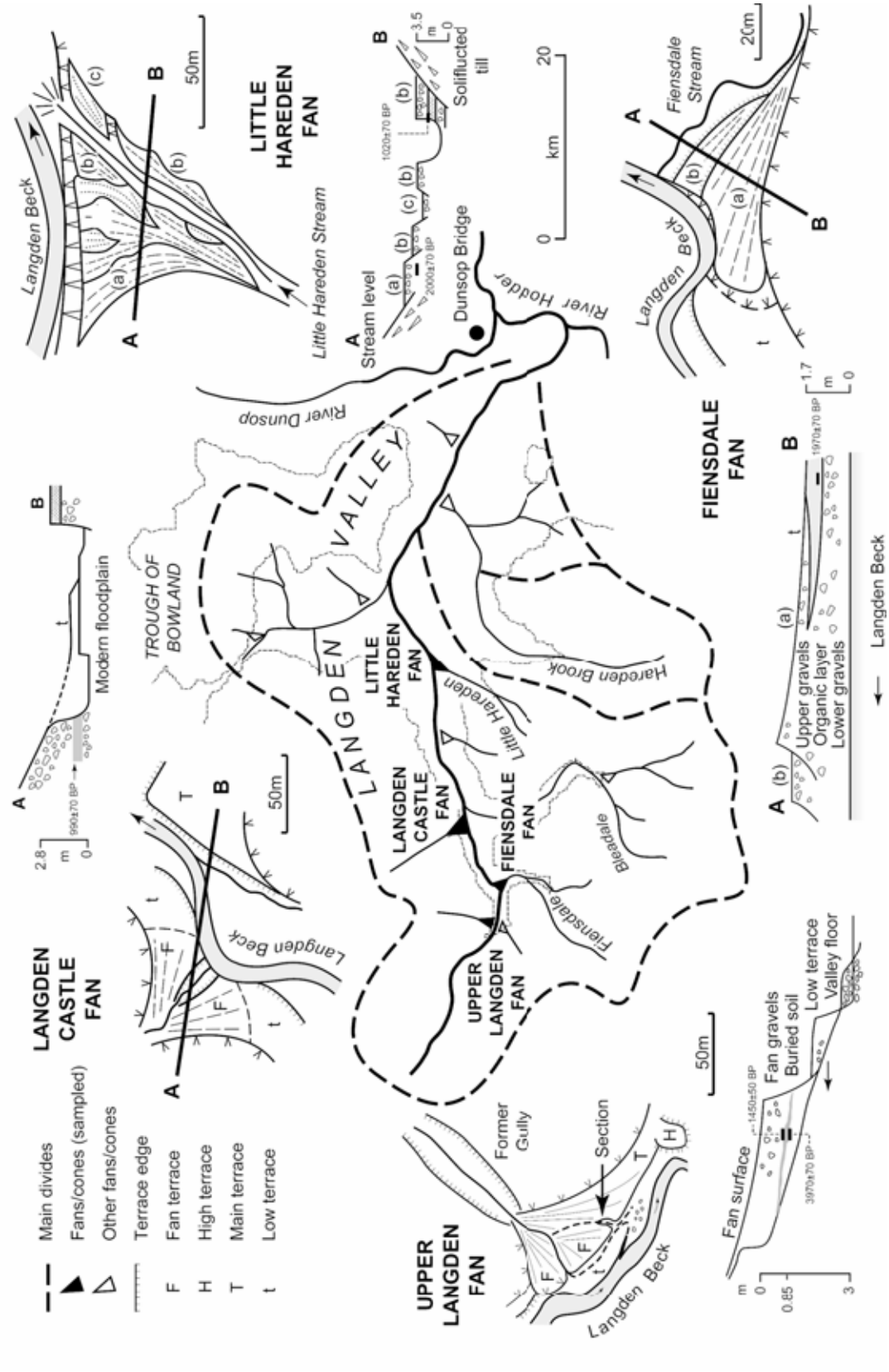

Figure 103: Geomorphological map of dated alluvial fan/gully sites in the Bowland Fells, Lancashire (Harvey and Renwick 1987; Chiverrell *et al* 2006)

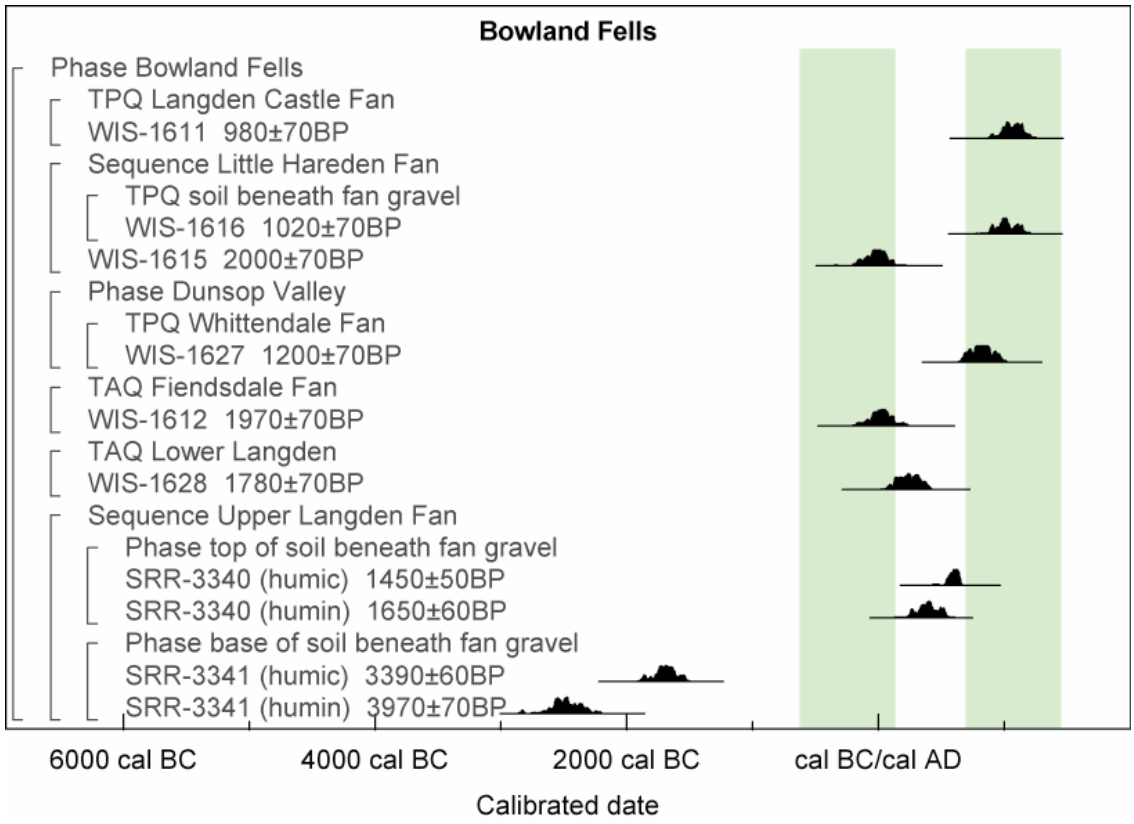

Figure 104: Probability distributions of dates from alluvial fan/gully sites in the Bowland Fells. Each distribution represents the relative probability that an event occurred at a particular time. These distributions are the result of simple radiocarbon calibration (Stuiver and Reimer 1993)

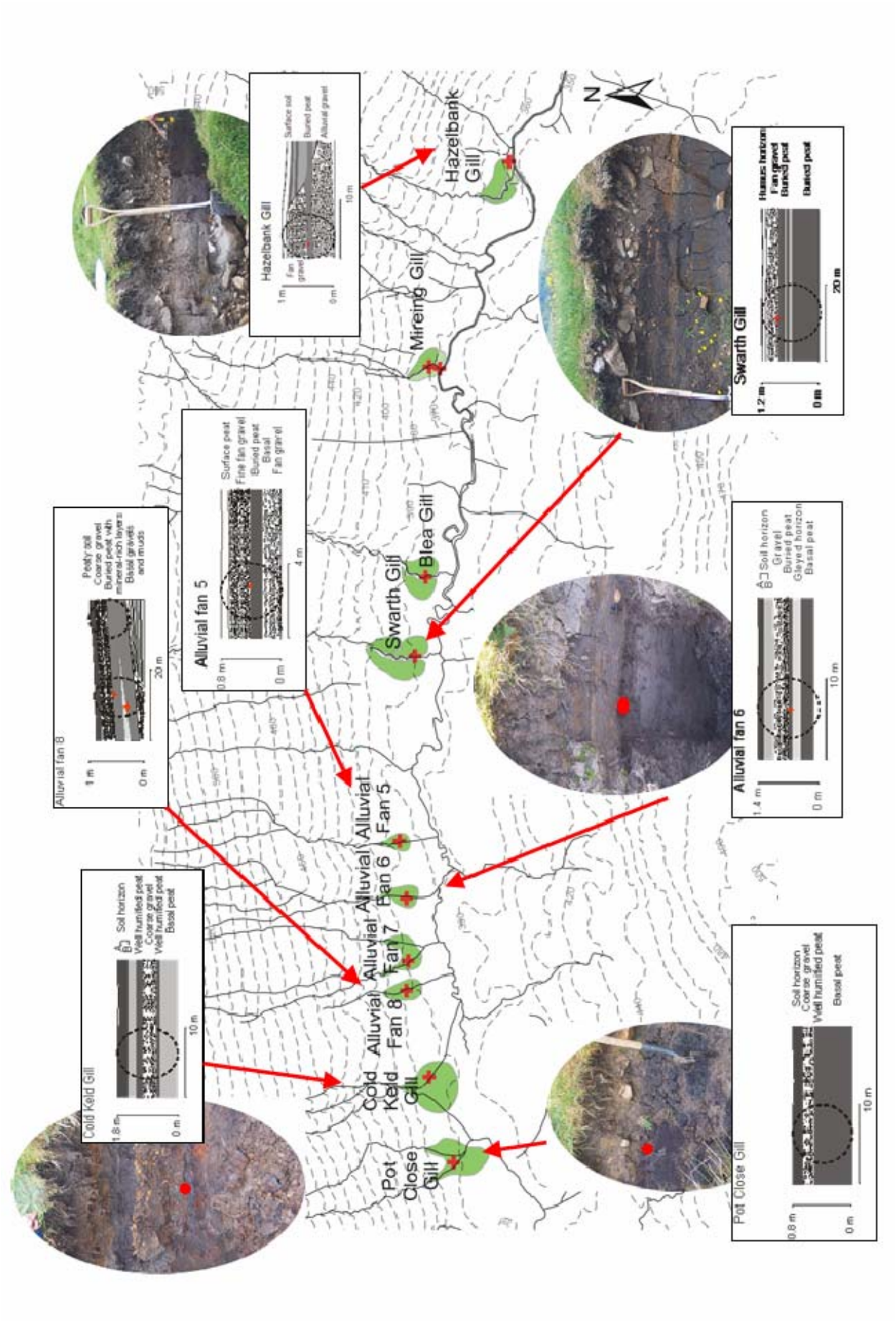

Figure 105: Geomorphological map of sampled alluvial fan/gully sites in the Ribble-Wharfe interfluve zone, Yorkshire

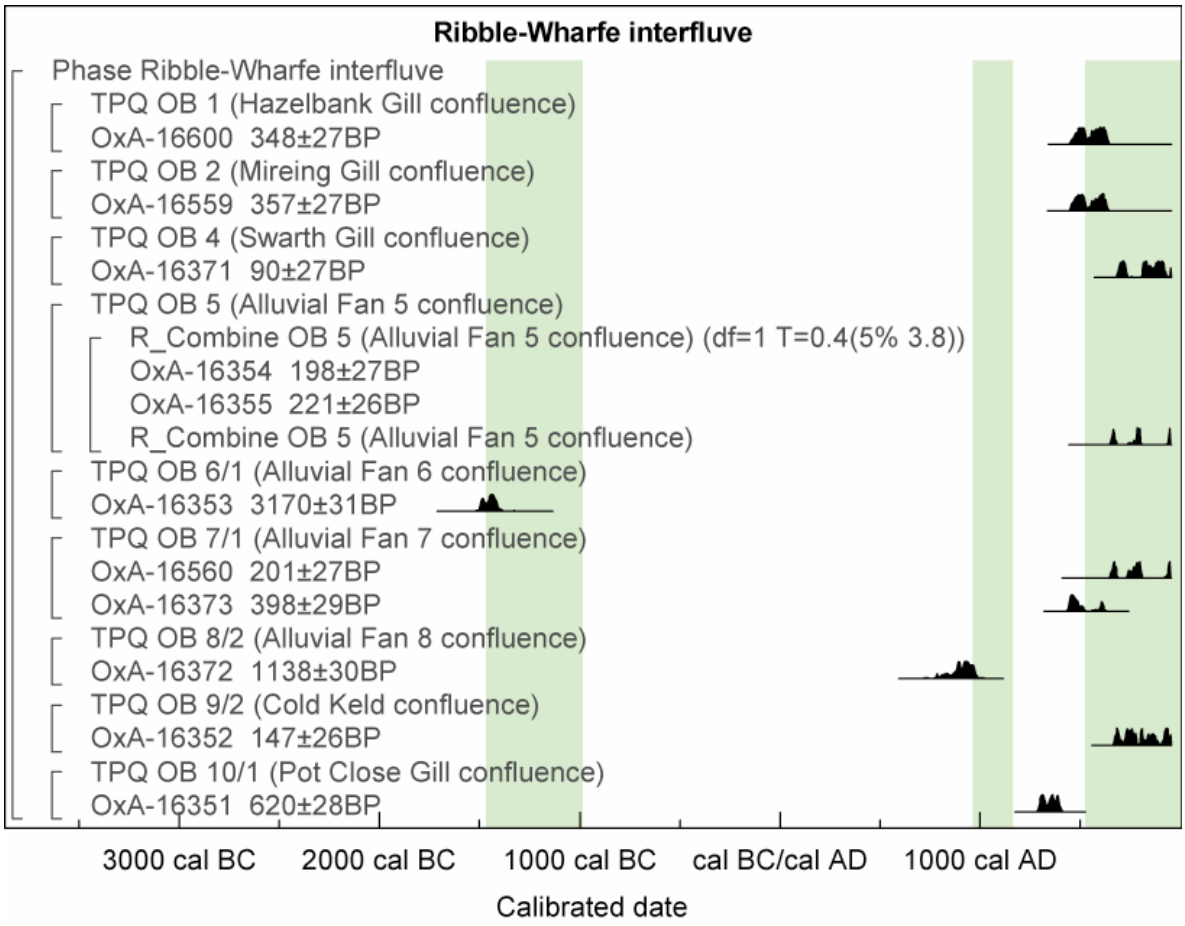

Figure 106: Probability distributions of dates from alluvial fan/gully sites in the Ribble-Wharfe interfluve. Each distribution represents the relative probability that an event occurred at a particular time. These distributions are the result of simple radiocarbon calibration (Stuiver and Reimer 1993)

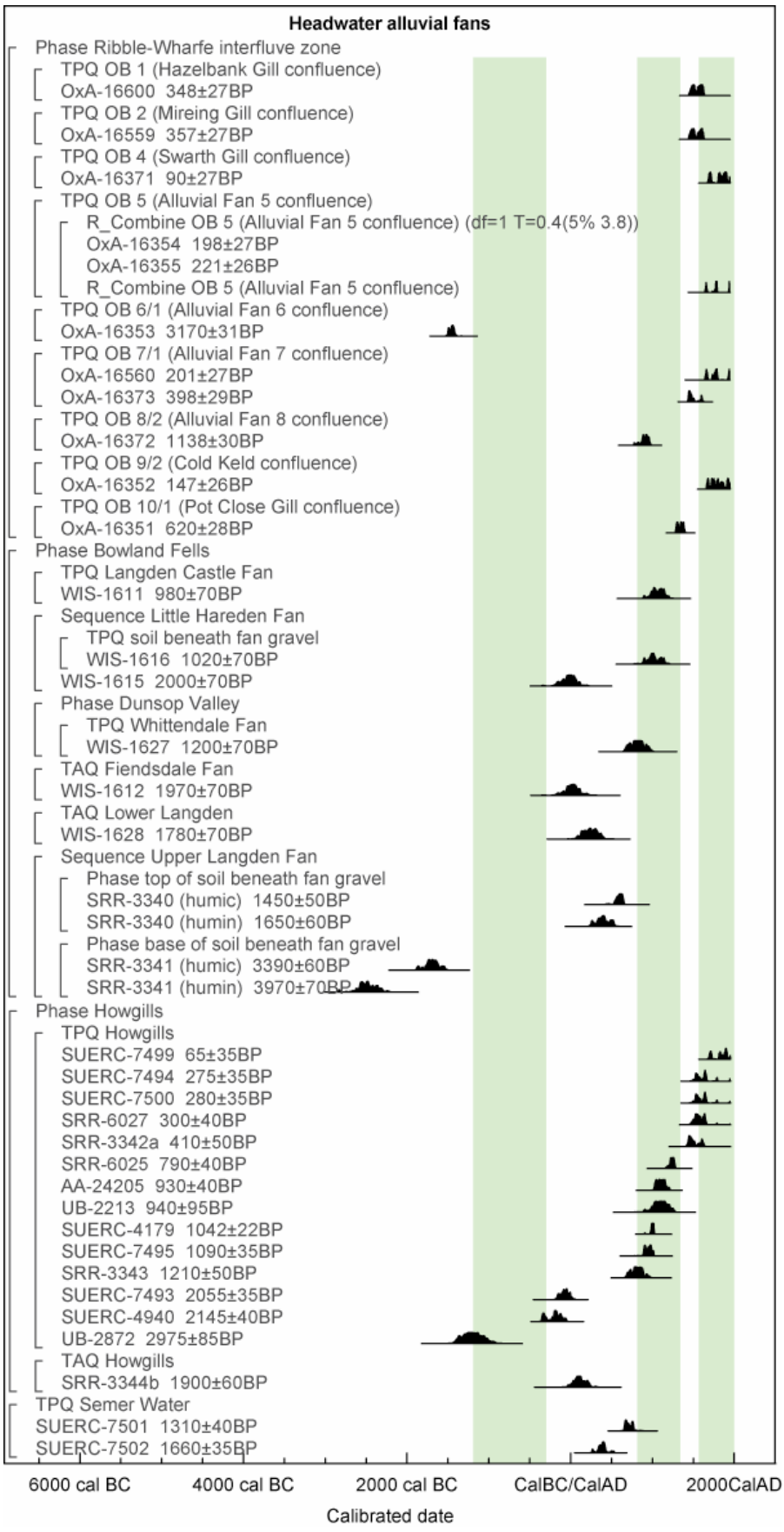

Figure 107: Probability distributions of dates from alluvial fan/gully sites in the Bowland Fells, Ribble-Wharfe interfluve, Howgills and Semer Water. Each distribution represents the relative probability that an event occurred at a particular time. These distributions are the result of simple radiocarbon calibration (Stuiver and Reimer 1993)

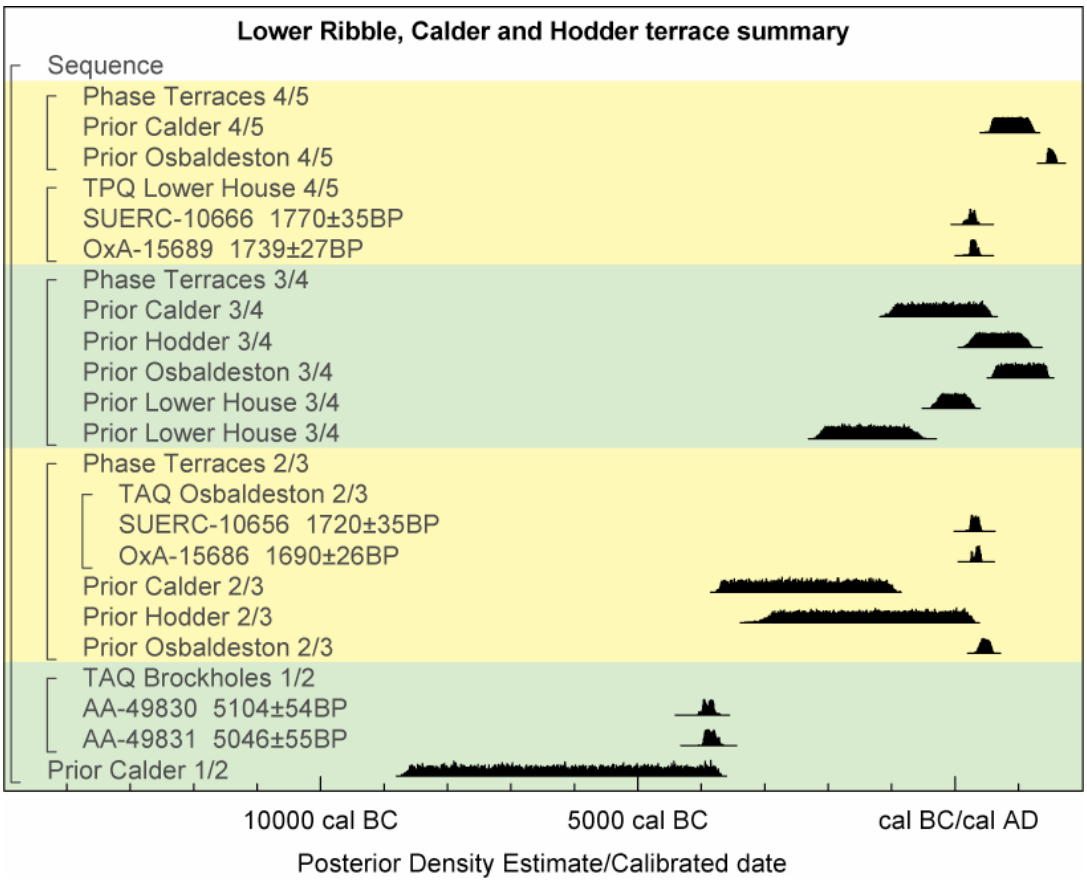

Figure 108: Chronological summary of main dated terrace events in the Lower Ribble, Calder and Hodder. Distributions labelled *Prior* have been imported from the models in Figures 76, 78, 86, 92, 94 and 102

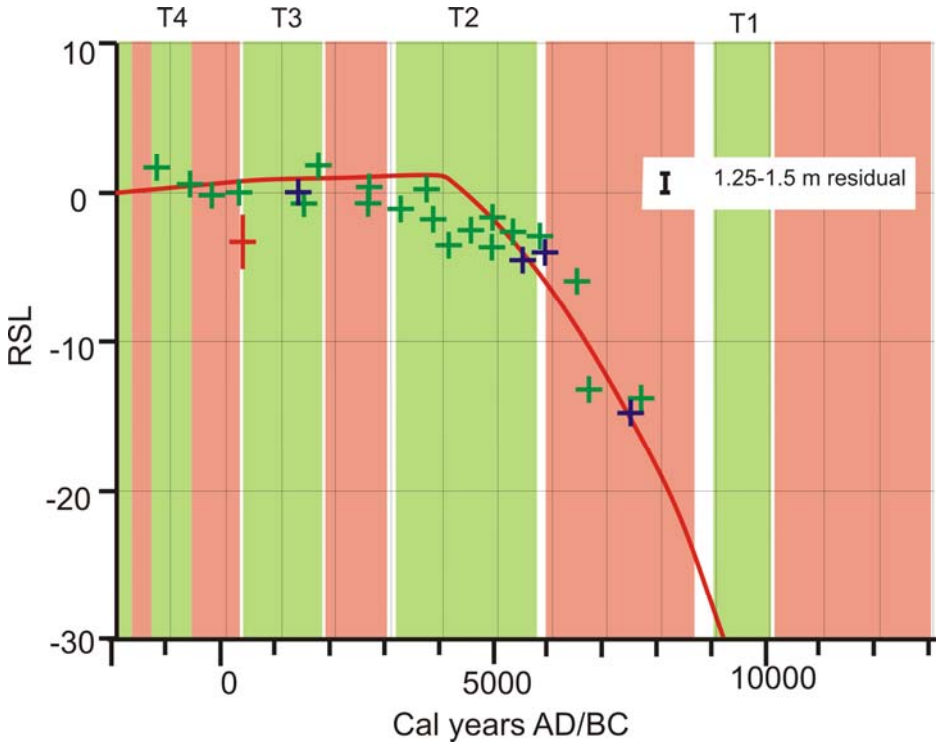

Figure 109: Comparison of Ribble fluvial development with green significant phases of aggradation and red incision episodes, and these are contrasted with the regional relative sea level (Shennan *et al* 2006)

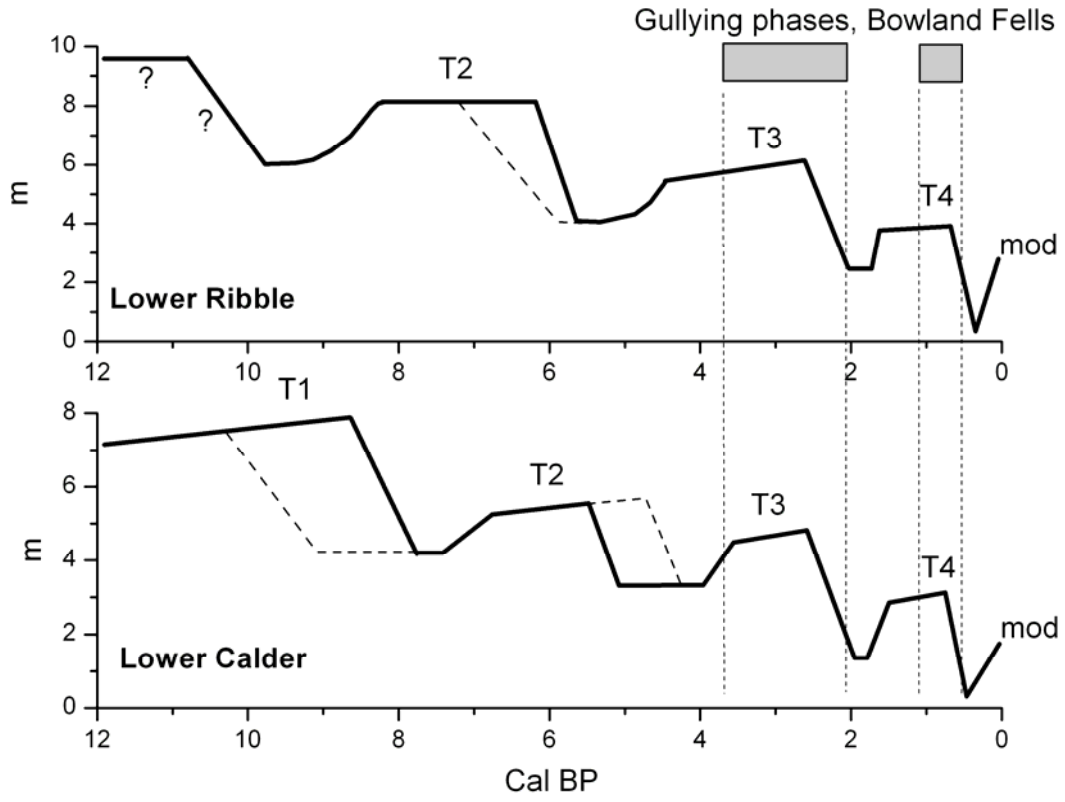

Figure 110: Comparison between the timing of hillslope gully/alluvial fan development in the Bowland Fells (source: Harvey and Renwick 1987) and river terrace development in the Ribble catchment

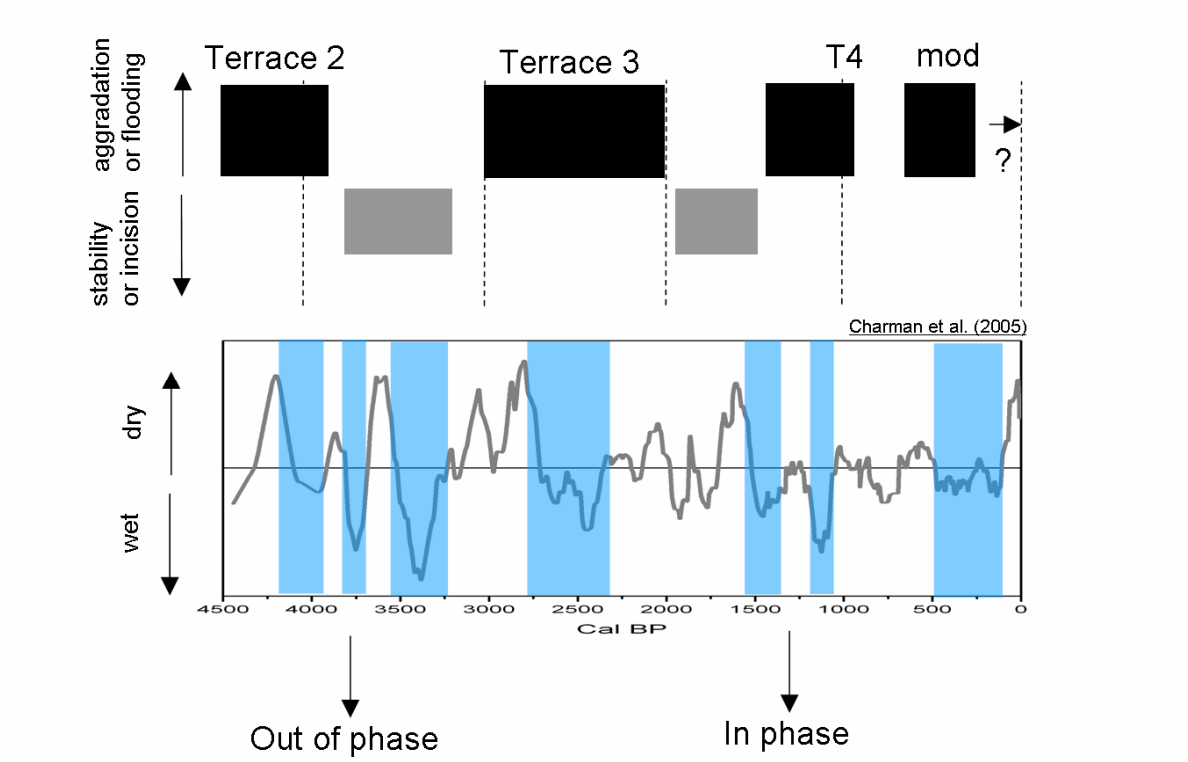

Figure 111: Comparison of terrace development in the Ribble catchment and north England bog surface wetness and reconstruction of regional hydroclimatic conditions (source: Charman *et al* 2005)

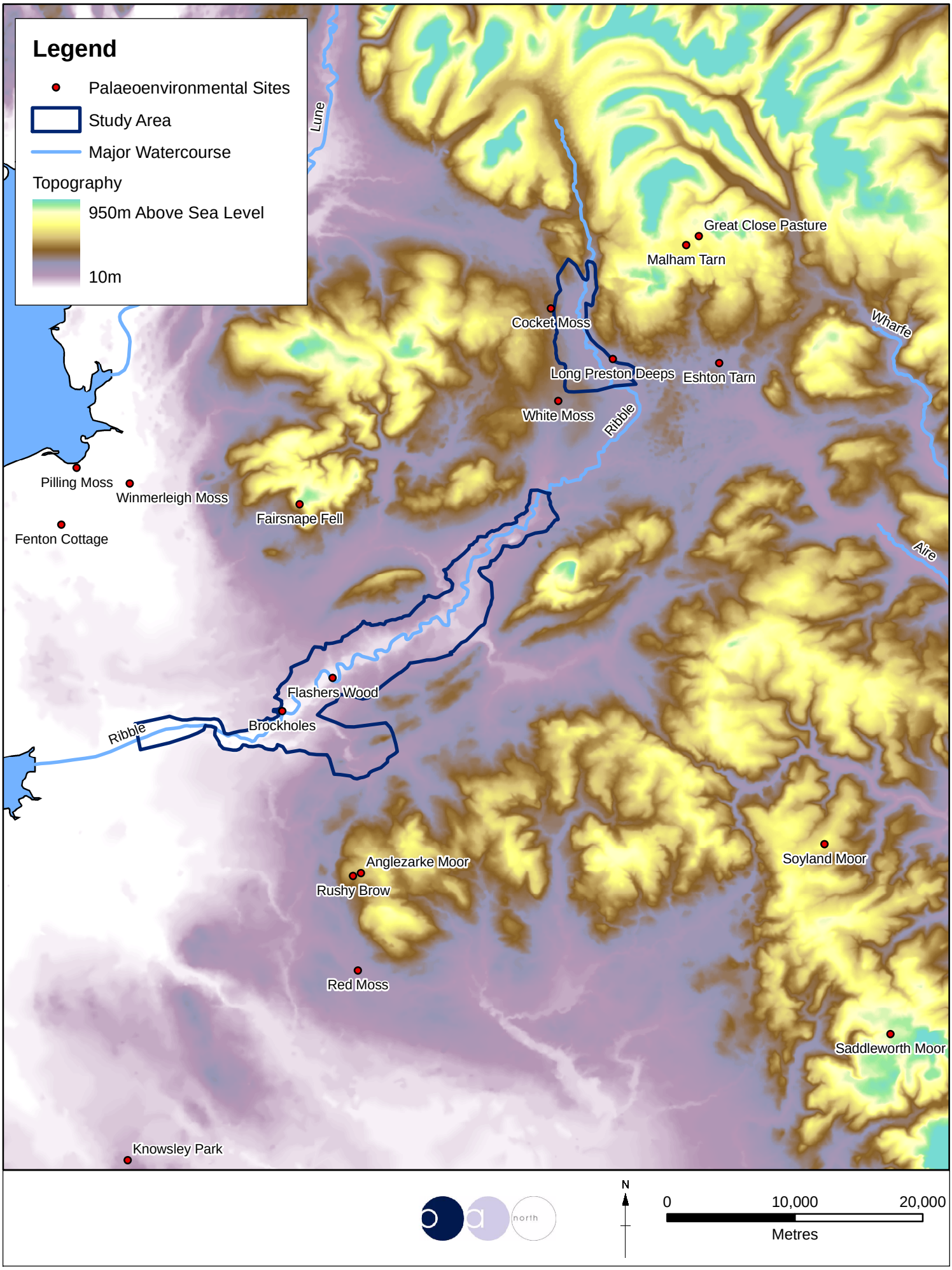

Figure 112: Palaeoenvironmental sites referred to in the text